

A SCANSORIAL VARANOPID EUPELYCOSAUR FROM THE PENNSYLVANIAN OF NEW MEXICO

SPENCER G. LUCAS

New Mexico Museum of Natural History and Science
1801 Mountain Road NW, Albuquerque, NM 87104
spencer.lucas@state.nm.us

LARRY F. RINEHART

New Mexico Museum of Natural History and Science
1801 Mountain Road NW, Albuquerque, NM 87104
larry.rinehart@earthlink.net

MATTHEW D. CELESKEY

New Mexico Museum of Natural History and Science
1801 Mountain Road NW, Albuquerque, NM 87104
matt.celeskey@state.nm.us

DAVID S BERMAN

Curator Emeritus, Section of Vertebrate Paleontology
Carnegie Museum of Natural History, 4400 Forbes Avenue, Pittsburgh, Pennsylvania 15213
berman@carnegiemnh.org

AMY C. HENRICI

Collection Manager, Section of Vertebrate Paleontology
Carnegie Museum of Natural History, 4400 Forbes Avenue, Pittsburgh, Pennsylvania 15213
henricia@carnegiemnh.org

ABSTRACT

An incomplete skeleton of a small tetrapod from the Upper Pennsylvanian of New Mexico represents a new genus and species of varanopid eupelycosaur named *Eoscansor cobrensis*. This skeleton is from the Cobrean (Virgilian) interval of the El Cobre Canyon Formation in the Cañon del Cobre of Rio Arriba County, New Mexico. *Eoscansor* is a small varanopid distinguished from other varanopids primarily by the unique structure of its manus and pes metapodials and phalanges. Diverse aspects of its anatomy indicate that *Eoscansor* was a climber, and possibly arboreal, the oldest such tetrapod now known. These features include: claw, phalangeal, and metapodial adaptations indicative of grasping, clinging, and climbing ability; equivalence of high claw curvature and limb length between the fore- and hind limbs; body mass per SVL within the range of extant climbing lizards; very low tibia length/femur length ratio; and a low center of gravity to facilitate an inclined surface-hugging posture.

KEY WORDS: Cañon del Cobre, eupelycosaur, New Mexico, Pennsylvanian, scansorial, varanopid

INTRODUCTION

The history of tetrapod arboreality (living in trees) has been long discussed, particularly with regard to the origins of birds, mammals, placental mammals, and primates (e.g., Matthew 1904; Haines 1958; Cartmill 1992; Feduccia 1999). *Anthracodromeus*, from the Middle Pennsylvanian of Linton, Ohio, is the oldest known tetrapod to possess incipient adaptations for climbing (Mann et al. 2021) in that it was capable of clinging to stumps and trees, but lacked adaptations for grasping. The first scansorial tetrapods to employ grasping are from the Permian of Russia and Germany (Fröbisch and Reisz 2009, 2011; Spindler et al. 2018). Here, we add to this early record of tetrapod locomotor modes an even older tetrapod climber that employed grasping, from the upper Carboniferous (Upper Pennsylvanian) of New Mexico, USA. This animal is a new genus and species of varanopid eupelycosaur named here. To establish its scansoriality (climbing), we provide diverse osteological criteria based on a review of skeletal traits indicative of and consistent with scansoriality in

living and extinct tetrapods, notably in lizards. The new varanopid named here is the oldest known scansorial tetrapod capable of grasping and contributes to the growing diversity and disparity of varanopid eupelycosaurs.

Abbreviations

LVF = land-vertebrate faunachron;
NMMNH = New Mexico Museum of Natural History and
Science, Albuquerque, New Mexico;
SVL = snout-to-vent length.

GEOLOGICAL CONTEXT

The skeleton described here was collected in the Cañon del Cobre (El Cobre Canyon), a large box canyon in south-eastern Rio Arriba County, northern New Mexico (Fig. 1). The canyon exposes ~ 450 m of siliciclastic red beds of Carboniferous–Permian age (Lucas et al. 2010b). These are nonmarine fluvial deposits of the Cutler Group—the

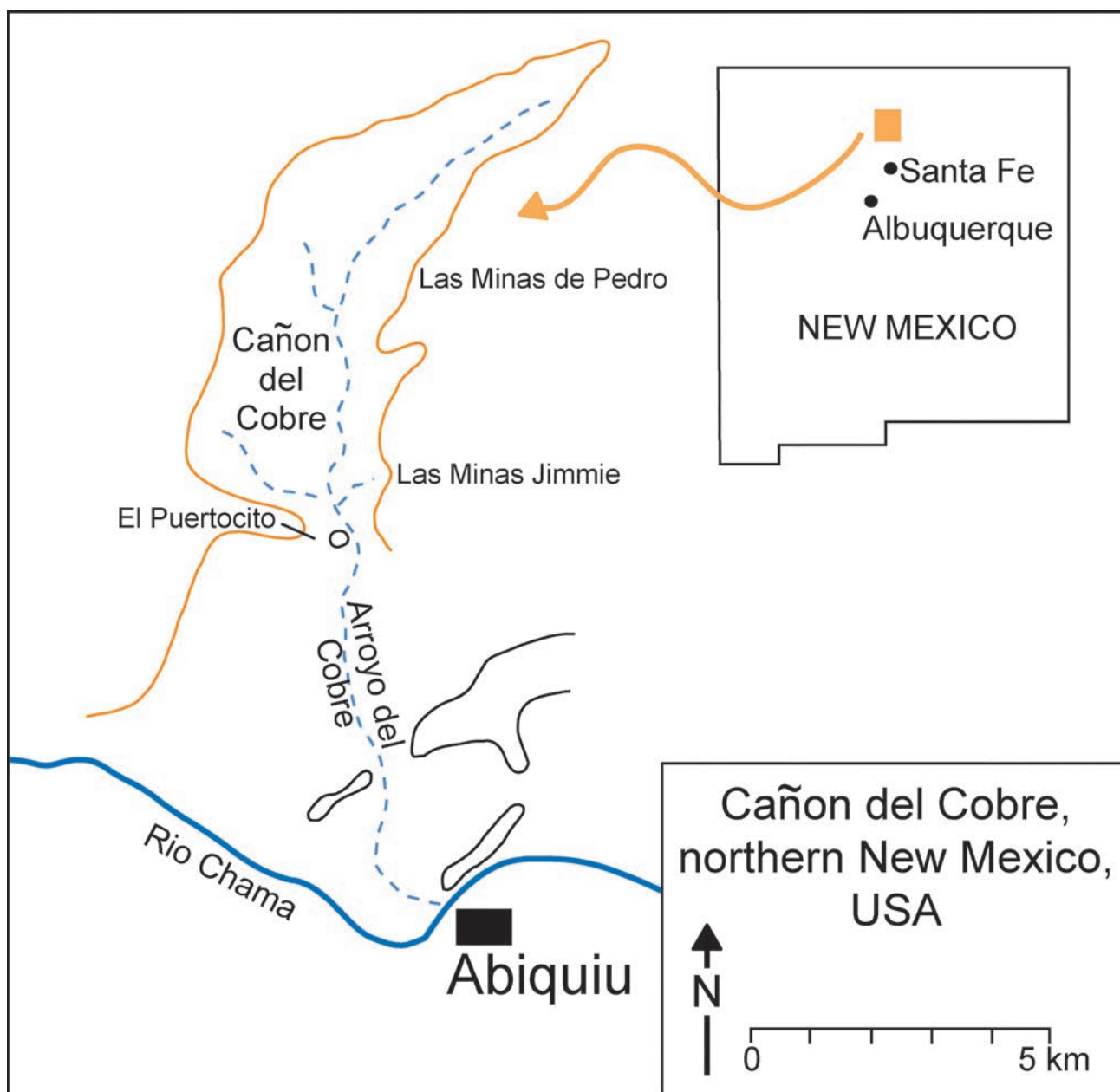


Fig. 1.—Index map showing location of Cañon del Cobre in northern New Mexico (modified from Lucas et al. 2010b)

upper part of the El Cobre Canyon Formation overlain by the Arroyo del Agua Formation (Lucas and Krainer 2005). These strata yield trace fossils, palynomorphs, macrofossil plants, and vertebrate fossils, some of which have been collected and studied since the 1870s (see articles in Lucas et al. 2010a).

In Cañon del Cobre, three stratigraphically superposed vertebrate fossil assemblages have been recognized (Lucas 2006, 2018; Lucas et al. 2010c) (Fig. 2). The oldest assemblage is characteristic of the Cobrean land-vertebrate faunachron (LVF) and comes from the lower 140 m of the

El Cobre Canyon Formation exposed in the canyon floor and along the lower walls of Cañon del Cobre.

This vertebrate fossil assemblage includes tetrapod taxa long known only from Pennsylvanian strata: *Desmatodon*, *Diasparactus*, and *Limnoscelis* (Vaughn 1963; Fracasso 1980; Lucas et al. 2010c). It is also co-extensive with an *Alethopteris* dominated macroflora considered to be of Late Pennsylvanian, likely Virgilian, age (DiMichele et al. 2010). Utting and Lucas (2010) considered palynomorphs from low in this stratigraphic interval to be Late Pennsylvanian. Therefore, Lucas et al. (2010c) considered

the Cobrean characteristic assemblage to be Virgilian in age, which is approximately co-eval with the Gzhelian Stage, ~ 299–304 Ma (Aretz et al. 2020). The skeleton described here was collected in about the middle of the stratigraphic interval of this assemblage, and thus is part of the characteristic assemblage of the Cobrean LVF of Late Pennsylvanian age (Fig. 2).

Above the Virgilian age assemblage, the 47 m thick interval of the upper part of the El Cobre Canyon Formation contains a second distinct assemblage. It is unfortunately low in diversity, but includes *Sphenacodon*, and thus was regarded as of Coyotean (latest Pennsylvanian–early Permian) age by Lucas et al. (2010c). The stratigraphically highest assemblage is from one locality 85 m above the base of the overlying Arroyo del Agua Formation and includes *Platyhystrix*, *Diadectes*, and *Sphenacodon* (Fig. 2). Correlative assemblages outside of the Cañon del Cobre include *Seymouria*, so this stratigraphically highest tetrapod assemblage in the Cañon del Cobre section is assigned a Seymouran (early Permian) age (Lucas et al. 2010c).

SYSTEMATIC PALEONTOLOGY

Synapsida Osborn, 1903
Eupelycosauria Kemp, 1982
Varanopidae Romer and Price, 1940

Eoscansor, new genus

Type species.—*Eoscansor cobrensis*.

Included species.—Only the type species.

Etymology.—From Greek *eo*, “dawn” and *scansor*, “climber,” in reference to the antiquity of this scansorial tetrapod.

Diagnosis.—A small varanopid (femur length ~ 22 mm) distinguished from other varanopids (except *Archaeovenator* and *Ascendonanus*) by its simple, somewhat laterally compressed, slightly recurved, and unserrated teeth. Among varanopids, in *Eoscansor* the following features of its manus and pes morphology are unique: manual and pedal ungual claws are relatively long, sharply pointed, laterally compressed, have large flexor tubercles and a relatively large curvature (~ 92°) of equal value in the manus and pes; elongate proximal and penultimate phalanges; a high phalangeal index (sum of proximal and penultimate phalangeal lengths as a percentage of the length of their associated metapodial); and the digit I metapodial is short with a wide proximal end. *Eoscansor* also differs from *Varanodon* by not having elongate cervical vertebrae, having a humerus longer than the radius, and a metatarsal IV that is shorter than the tibia. *Eoscansor* lacks the short and stout forelimb and long ungual phalanges characteristic of *Mesenosaurus*. The greatly elongated manus and pes ungual phalanges with slender flexor tubercles of *Tambacarnifex* also distinguish it from *Eoscansor*, and the long

presacral vertebral column of *Ascendosaurus* also distinguishes it from *Eoscansor*.

Eoscansor cobrensis, new species

Holotype.—NMMNH P-75122, incomplete skeleton consisting of skull fragments, an incomplete dentary with seven teeth, atlas, axis, two anterior cervical vertebrae, at least ten dorsal vertebrae, two sacral vertebrae, eight caudal vertebrae, incomplete interclavicle, parts of both clavicles, assorted ribs and gastralia, humeri, right radius, ulnae, partial left and right manus, left ilium, ischium, pubis, femora, tibiae, fibulae, and incomplete left and right pedes.

Type locality.—NMMNH locality 6121A, El Cobre Canyon Formation in Cañon del Cobre, Rio Arriba County, New Mexico, USA (Figs. 1–2). Map coordinates of this locality are on file in the NMMNH database and are available to qualified researchers.

Etymology.—Cobrensis, for the type locality in Cañon del Cobre (El Cobre Canyon), New Mexico.

Diagnosis.—As for the genus.

DESCRIPTION

General

The fossil is preserved as part and counterpart on two blocks of rock, here referred to as block A and block B (Figs. 3–6). The sediment of both blocks is a slightly sandy siltstone that is grayish red (5R4/2) to grayish red purple (5P4/2). In places it has a patchy weathering rind that is pale reddish brown (10R5/4).

Block B exposes much of the skeleton in dorsal view (Figs. 5–6). An additional small block that fits on block B was found at the locality (Fig. 7). This block contains numerous fragmented skull bones, a dentulous jaw fragment, atlas, axis, and two subsequent cervicals in articulation, and parts of an interclavicle and both clavicles, also articulated (Fig. 7). The remainder of block B preserves some of the dorsal vertebrae, part of the caudal vertebral series, the left ilium, various ribs and gastralia, both humeri, an ulna, part of the left radius, much of the right manus, both femora and tibiae, the left fibula and parts of the right and left pedes. Block A (Figs. 3–4) preserves more of the tail than B, less of the manus and pedes, but more of the long bones, as they are mostly impressions in block B. Measurements of the bones on blocks A and B are in Table 1.

The holotype of *Eoscansor cobrensis* appears to be an immature individual based on the lack of fusion between the vertebral neural arches and centra. Furthermore, the carpal and tarsal bones are not preserved and presumably were not ossified at the time of death.

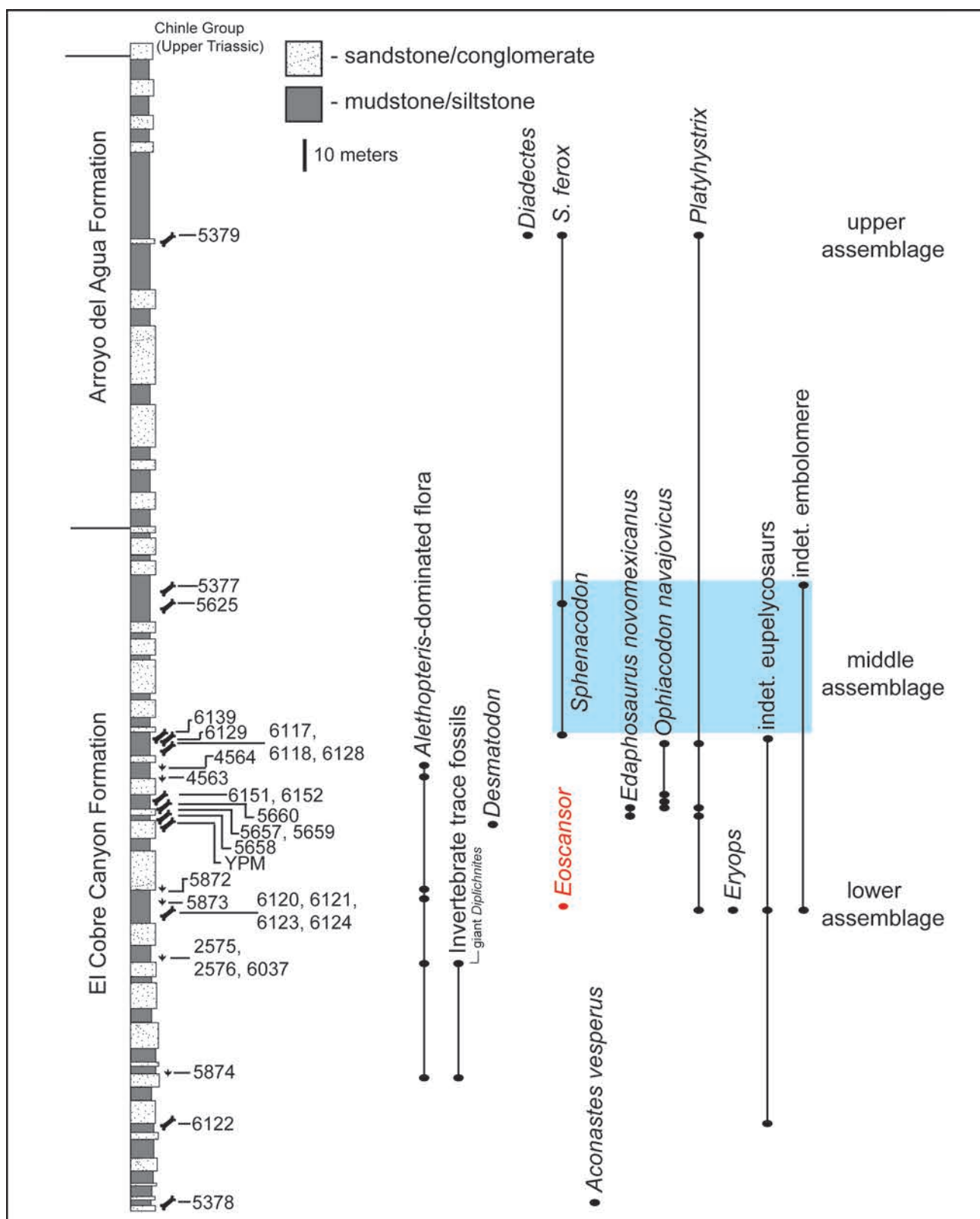


Fig. 2.—Stratigraphic distribution of NMMNH fossil localities (numbers on left) and taxa in the Cañon del Cobre (modified from Lucas et al. 2010c).

Skull, Lower Jaw and Dentition

The portion of block B that contains a jaw fragment also includes some flat, fragmented bones (Fig. 7). These are almost certainly cranial, but they are too poorly preserved to provide useful anatomical information.

An incomplete portion of the apparently long and slender left lower jaw is present bearing parts or all of seven teeth that are part of a single marginal row. The lateral surface of the lower jaw is broken, exposing the teeth and their roots. The teeth are similar to each other in shape—as simple, nonserrated, somewhat laterally compressed crowns with slightly recurved and pointed tips, and cylindrical roots with subthecodont implantation. The tooth crowns are somewhat laterally compressed and have an elliptical cross section. The anteriormost two teeth and the fourth tooth are larger than the other teeth. The third tooth is a broken fragment. Tooth length at the crown base is ~1 mm in the first, second, and fourth teeth, but only about 0.6 mm in the last three teeth.

Vertebral Column

The incompletely preserved vertebral column of NMMNH P-75122 consists of the atlas, axis, and two postatlantal cervicals, four anterior dorsals, three posterior dorsals, two sacrals, and eight caudals. The best preserved and most complete of these are the cervicals and the caudals. All of the centra are relatively short and blocky (about as wide as long) and slightly waisted midlength, so as to have a spool shape. All appear to be amphicoelous, whereas a few are notochordal, indicating that they have deeply conical articular ends. Except for the cervicals and a caudal, none of the vertebrae have neural arches, and on the better preserved caudal centra, it is clear that the neural arches were not fused to the centra.

Four cervical vertebrae, including the atlas and axis, are preserved articulated with their left sides lying against the dorsal surface of the interclavicle (Fig. 7). The centra are short and about as long as they are tall. The proatlas, atlantal intercentrum, and most of the atlantal neural arch are missing. The atlantal pleurocentrum has articular facets for the neural arch on its anterior dorsal surface and displays a lateral excavation similar to what Campione and Reisz (2011) reported in *Varanops*. The pleurocentrum extends ventrally to the ventral edge of the axial centrum, presumably preventing contact between the atlantal and axial intercentra. The axial centrum is short with an anteroposterior length only slightly longer than that of the atlas. The axial neural spine is more than twice the height of the centrum with a rounded dorsal edge. It is inclined anterodorsally, extending beyond the level of the anterior margin of the centrum. The width of the neural spines narrows on the third and fourth cervicals so that only the zygapophyses extend beyond the margins of the centrum. Transverse processes of the axis and the third cervical vertebrae end in laterally facing, subcircular articular facets.

The proximal end of the right axial rib is slightly displaced below the articular facets of the transverse process and the axial intercentrum.

Preserved on block A are three dorsal centra just posterior to the gastralria (Figs. 3–4) that are articulated to one another and closely associated to their dorsal ribs on the right side. The centra are about as long as they are wide. Neural arches are not preserved (or are buried in the matrix), and the ribs articulate at the contact between the centra. Portions of one anterior dorsal well separated from at least two anterior dorsals on block A (Figs. 3–4) are near the preserved portions of the humeri. The two (or more) centra have been crushed onto each other and reveal no additional morphological information than the three posterior dorsal centra on that block.

On block B (Figs. 5–6), parts of three posterior dorsal vertebrae have centra that are longer than those of the anterior dorsals, giving these posterior dorsal centra a more rectangular (longer than wide) shape (they could be lumbars). The posterior dorsals have much thinner, shorter ribs with larger articular ends than do the anterior dorsal vertebrae. Two sacral vertebrae are preserved, one on block A and the other on B (Figs. 3–6). These vertebrae have blocky centra, best seen in block B.

A string of caudals is exposed as counterparts in which the ventral half of each centrum is preserved in block A and the dorsal half of each centrum with neural arch (embedded in matrix) is preserved in block B. One of the well-exposed caudal centra on block A (Figs. 3–4) has an amphicoelous posterior articular surface. This caudal also has three antero-posteriorly aligned ridges on its ventral surface, one a medial ridge flanked by two lateral ridges. Neural arches are mostly buried in the matrix except for one caudal exposed in lateral view. A thin neural spine extends posteriorly beyond the posterior end of the centrum of this caudal.

The caudal vertebrae have short, curved ribs with thick, cap-like articular surfaces to meet the centra. There are two visible isolated haemal arches that are tall and have a narrow v-shape cross section. The proximal articular surface of the haemal arch is wide and nearly flat.

Ribs and Gastralria

There are relatively few ribs preserved in NMMNH P-75122. However, they do show that *Eoscaenops* had cervical, anterior dorsal, posterior dorsal, and caudal (at least anterior caudal) ribs. Parts of three cervical ribs are preserved on block B (Figs. 5–6). All lack their proximal ends and are relatively short, flexed, and have pointed distal tips.

Parts of at least eight dorsal ribs, all incomplete, are present. These ribs are thin and gently curved, with grooved dorsal and ventral surfaces. Their proximal articulations possess a distinct tuberculum and capitulum. The tuberculum is larger than and extends more proximally



Fig. 3.—Photograph of NMMNH P-75122, holotype of *Eoscaenops cobrensis*, block A.

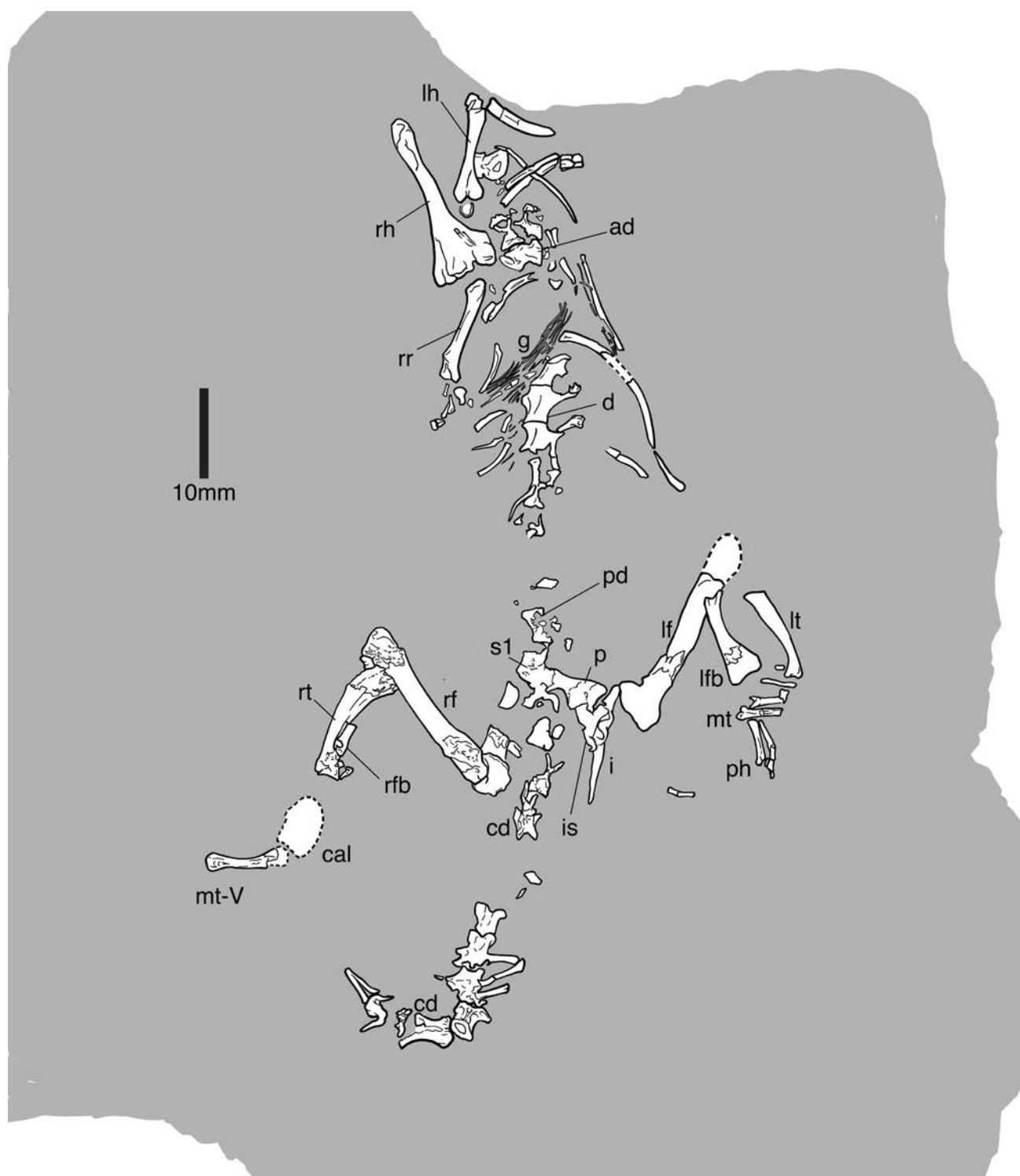


Fig. 4.—Bone map of NMMNH P-75122, holotype of *Eoscansor cobrensis*, block A. Abbreviations: ad = anterior dorsal vertebra, cal = calcaneum, cd = caudal vertebra, d = dorsal vertebra, g = gastralria, i = ilium, is = ischium, lf = left femur, lfb = left fibula, lh = left humerus, lt = left tibia, mt = metatarsal, p = pubo-ischiatic plate, pd = posterior dorsal vertebra, ph = phalanx, rf = right femur, rfb = right fibula, rh = right humerus, rr = right radius, rt = right tibia, s1 = first sacral vertebra.

than the capitulum.

On block B some of the posterior dorsal vertebrae (possibly lumbars) have short and nearly straight ribs. The caudal ribs visible on block A (Fig. 3) are narrow and arcuate in dorsal/ventral view, and the proximal articulation is a broad, cup-like structure.

Numerous gastralia are preserved on blocks A and B (Figs. 3–6). They are very thin, almost hair-like bones a few mm long that were presumably positioned in metamerid rows between the pubis and sternum (cf. Claessen 2004).

Interclavicle

The interclavicle is present on the small “skull” block that fits on block B (Fig. 7). In dorsal aspect, it is about 15 mm wide and has a smooth surface. It is mostly covered by the clavicles anteriorly and laterally and by the first four articulated cervical vertebrae posteriorly.

Clavicle

Paired clavicles are present on the small “skull” block as arcuate bones. The left clavicle is slightly damaged, but impressions in the matrix clearly define the missing parts. The right clavicle is more severely damaged and is missing much of its lateral edge. Seen in dorsal view, they are convex ventrolaterally with a smooth, arcuate lateral edge. The clavicles are approximately 16 mm long, and their posterior terminus is sharply pointed.

Scapulo-coracoid Complex

What appear to be portions of the scapulo-coracoid complex are preserved on block B (Figs. 5–6). They closely resemble those of other eupelycosaurs (Romer and Price 1940). The scapular blade is displaced from the remainder of the scapulocoracoid complex. In medial view the scapula is a long, strap-like bone that is slightly bowed (concave). The blade has a slightly widened distal end, and its broken medial end is also slightly widened.

The scapulo-coracoid also includes a nearly complete coracoid that has a nearly round outline in lateral view and an attached proximal portion of the broken scapula blade. The coracoid plate thickens to a proximodistally oriented, low ridge that divides a larger anterior coracoid from a smaller posterior coracoid.

Humerus

The humerus of *Eoscaenops* exhibits the primitive tetrahedral morphology typical of most late Paleozoic tetrapods in having greatly expanded proximal and distal heads that are separated by a short cylindrical shaft and twisted about the long axis of the shaft to occupy nearly right angle planes to one another. The right humerus is nearly complete

and exposed in ventral view on block A (Figs. 3, 4, 8A), and a portion of the mid-region of the left humerus is preserved nearby. In block B (Figs. 5–6) the left humerus is preserved in dorsal aspect, and the right humerus is exposed in ?medial aspect. Note that the proximal end of the left humerus in block B is preserved on the small, separate piece of rock (Fig. 7), which is not included in Figs. 5–6.

The right humerus has a small hemispherical proximal articular surface that is only slightly wider than the shaft. The shaft has a trihedral cross section because of the prominent deltopectoral crest along its ventral surface. Distally, the shaft expands dramatically into a broad and nearly triangular distal end (in ventral view). Although it has been compressed dorsoventrally and fractured, the distal end preserves a proximodistally elongate entepicondylar foramen just distal to the point of expansion. The entepicondyle flares out from the humeral shaft much more than does the ectepicondyle. It has a proximal edge that is concave proximally, and its medial edge is partly obscured. Although the medial edge of the humerus in block B reveals the shaft to be a long and thickened surface (supinator process) for the attachment of flexor muscles, no ectepicondylar foramen is visible. The distomedial edge of the humerus has a concave trochlea but no capitellum lateral to it.

Radius

On block A, the right radius (Figs. 3–4) is preserved, nearly complete, and has been displaced so that it is not articulated to the humerus. This radius, although long and slender, is shorter than the humerus, and it has slightly expanded proximal and distal ends. The shaft is circular in cross section.

Ulna

On block B, both ulnae are preserved (Figs. 5, 6, 8A) in nearly their correct articulated position with the distal ends of their respective humeri. The ulna has a slightly curved shaft that is flattened dorsoventrally and an expanded, block-like distal end. The semilunar notch is shallow, and the olecranon process is short and blunt.

Manus

Part of the left manus is preserved on block A, and part of the right manus is on block B. Both are incomplete, disarticulated, and no carpal bones are preserved in either manus. The more complete right manus is on block B (Figs. 5, 6), but our reconstruction of the manus (Fig. 9) is based on the bones of both blocks A and B.

The bones of the manus are jumbled, so a phalangeal formula cannot be determined. Four broken, long, and cylindrical metacarpals are preserved (Fig. 9A). Their proximal ends are flat to slightly concave, and their convex distal ends articulate with the proximal phalanges.

This manus also preserves a very long digit that consists of four articulated phalanges with the distalmost being the ungual claw (phalanx), which we identify as the third digit. Other than this claw, the phalanges are long, thin, cylindrical bones with slightly expanded proximal and distal ends. The proximal ends have slightly concave articular surfaces, whereas the distal ends are slightly convex. The ungual is short and laterally compressed and has a curved bony claw with a prominent flexor tubercle. The three distal phalanges are closely articulated, revealing a penultimate phalanx that is much longer than the preceding phalanx (Table 1).

Ilium, Ischium, and Pubis

The left ilium is present and preserved in an upright, near-life position on block.

In dorsal view in block A (Figs. 3–4), it appears as a thin, blade-like bone lying parallel to the vertebral column. In lateral view, it shows only a large, curved posterior process. This process is much longer than wide, and is dorsoposteriorly curved over its entire length. Proximally, a cup-shaped feature represents the dorsal portion of the acetabulum.

The anterior medial edge of this ilium is slightly displaced from the pubo-ischiatic plate, and both the ilium and the pubo-ischiatic plate are overlapped by a triradiate bone fragment that may be part of the ischium. The pubo-ischiatic plate has a concavity along its posterior aspect that may be part of a fenestra (obturator foramen).

Additional fragments of the left pelvis are seen on block B (Figs. 5–6). The left pubis and ischium are preserved adjacent to the proximal end of the left femur and are exposed in dorsal aspect. Both are incomplete, but the rim of the acetabulum is visible.

Femur

Both femora are present, parts of which are present on both blocks A and B (Figs. 4, 6). As in most tetrapods, the *Eoscaenops* femur is the longest limb bone (Table 1). It is best preserved on block B, where most of the left femur can be seen in both lateral and posterior views (Figs. 5, 6, 8C). On block A, the distal end of the left femur is represented by broken bone and impression (dashed line in Fig. 6). Both femora have left thin skins of compact external bone on their respective counterpart blocks (left on B, right on A).

The proximal end of the femur includes the articular facet for the acetabulum and an internal trochanter, which are separated by a deep narrow intertrochanteric fossa. The proximal articular surface is an arcuate ridge that forms a relatively narrow flange with convex margins. The internal trochanter is a small, rounded process well distal to the proximal articular surface.

The femoral shaft is robust, and on block A the shaft of the left femur can be seen to be slightly curved (bowed)

so as to be slightly concave posteriorly. The distal ends of both femora are not completely preserved, but have two slightly expanded condyles for articulation with the tibia and fibula. The lateral condyle is larger than the medial condyle, but there is no substantial offset of the condyles proximodistally; instead, they are nearly in the same plane with respect to their tibial articulation. The two condyles are separated by a very shallow, narrow intercondylar fossa.

Tibia

The tibiae are much shorter than the femora (Table 1). The right tibia is best exposed and is essentially complete in block A (Figs. 3–4), and the nearly complete left tibia is well preserved on block B (Figs. 5–6, 8C). The counterparts to the tibiae are preserved, but are much more damaged. The tibia has a very broad proximal end that tapers very rapidly to a much narrower shaft and distal end. The shaft of the tibia is subcircular in cross section and markedly curved, so that the bone is concave laterally (toward the fibula). There is also a prominent blade-like cnemial crest on the anterior face of the shaft. The distal end of the tibia is wider than the shaft and appears as a convex flange of bone.

Fibula

The left fibula is preserved mostly on block A, and its counterpart is on block B (Figs. 3–4). Part of the greatly damaged right fibula is preserved on block B. The fibula of *Eoscaenops* has a narrow proximal end with a small depression on its lateral side that is the articular surface for the lateral condyle of the tibia. The fibula has a narrow, curved shaft that laterally is nearly flat, but concave medially (towards the tibia). The distal end is a broad, triangular flange of bone.

Pes

Block A has bones of the pedes, but they are incomplete and disarticulated (Figs. 3–4). A large calcaneum was once present on block A (Fig. 4), but it was damaged during study. Block B contains most of the elements of the right pes (Figs. 5–6, 10). One element, located near the distal end of the right fibula on block B, is much shorter than the others and has a very expanded proximal end. This is likely the first metatarsal. Three other elements on block B represent metatarsals II–IV. Near the fourth metatarsal is a partially articulated series of fragments and impressions of four elongate elements and a partial ungual. The longest of these impressions corresponds to the largest pedal bone remaining on block A, which we identify as metatarsal V. It is a long, cylindrical bone with a slightly expanded distal end that is a trochlea for articulation with the proximal phalanx. In addition to the metatarsals, digits I–IV are



Fig. 5.—Photograph of NMMNH P-75122, holotype of *Eoscansor cobrensis*, block B.

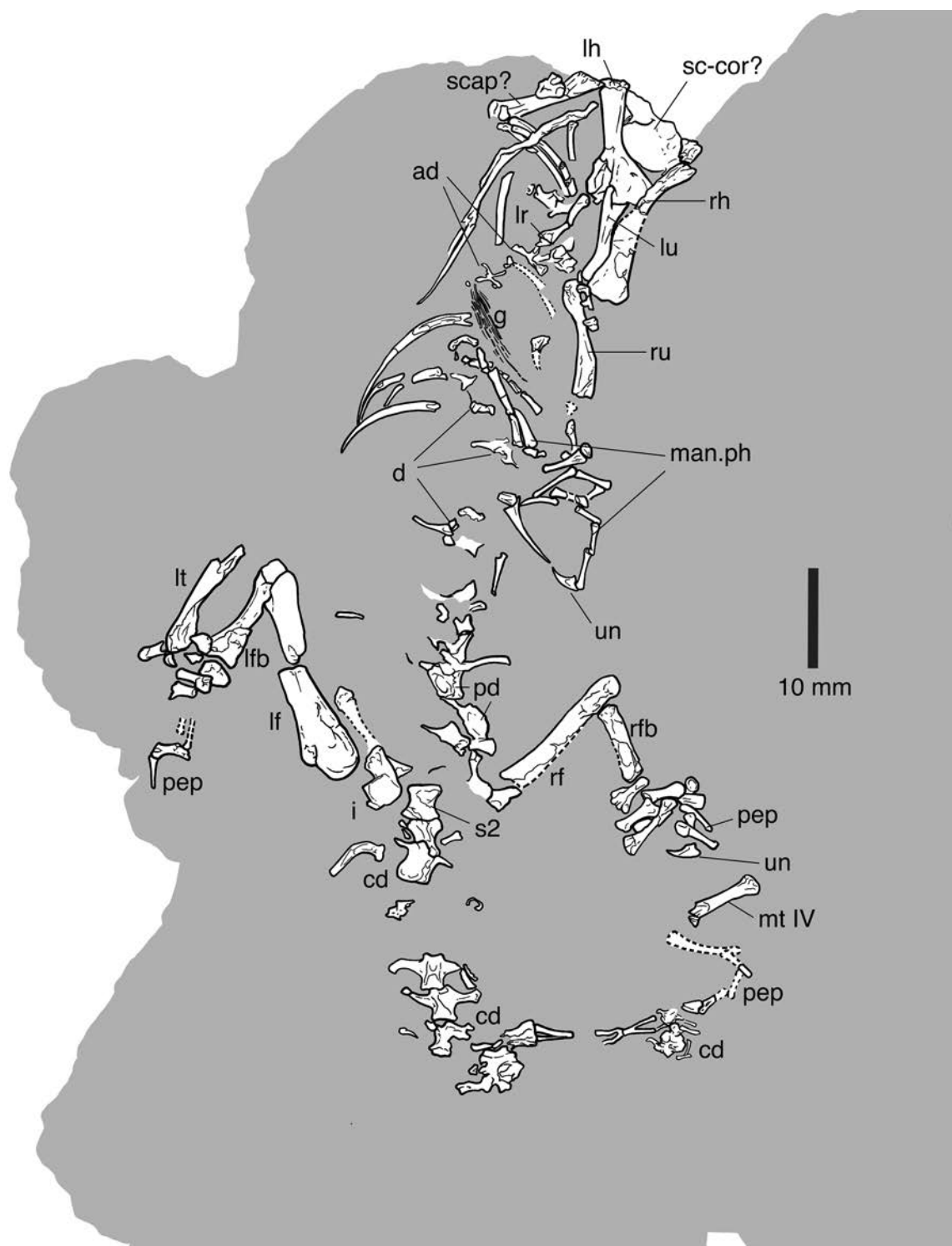


Fig. 6.—Bone map of NMMNH P-75122, holotype of *Eoscansor cobrensis*, block B. Abbreviations same as in Figure 3 with the following additions: lu = left ulna, man.ph = manual phalanges, pd = posterior dorsal vertebra, pep = pedal phalanges, ru = right ulna, scap? = scapula?, sc-cor? = scapula-coracoid?, un = ungual phalanx.

TABLE 1. Measurements (in mm) of NMMNH P-75122, holotype of *Eoscansor cobrensis*. est = estimate, inc = incomplete.

BODY	SVL	TAIL L	TOTAL L		
	125 est	120 est	245 est		
SHOULDER	Scap-cor L	Prox W	Mid-shaft W	Dist W	
	16.5	8.3	1.8	5.7	
FORELIMB	Humerus L	Prox W	Mid-shaft W	Dist W	
H+R=33.3	19.9	2.7	1.63 X 1.78	9.3	
	Radius L	Prox W	Mid-shaft W	Dist W	
	13.4	~ 1.8	0.93 X 1.4	2.5	
	Ulna L	Prox W	Mid-shaft W	Dist W	
	18.8				
Manus digit III	MC L	Phx1 L	Phx2 L	Phx3	Ungual L
	3.95	3.9	3.1	4.1	3.8
HIND LIMB	Femur L	Prox W	Mid-shaft W	Dist W	
F+T=36.5	22.4	~4.4	1.85	2.9	
	Tibia L	Prox W	Mid-shaft W	Dist W	
	14.1	3.5	2	1.8	
	Fibula L	Prox W	Mid-shaft W	Dist W	
	11.9	2.2	1.4	4.2	
PES	MT1 L	Prox W	Dist W		
	4.6	2.8	1.3		
	MT2 L	Prox W	Dist W		
	5.2	1.9	1.9		
	MT3 L	Prox W	Dist W		
		2.2			
	MT4 L	Prox W	Dist W		
	7.5	2.1	2.0		
	MT5 L	Prox W	Dist W		
	8.6	2.4	2.0		
PES DIGIT 5	Phx1 L	Phx2 L	Phx3 L	Ungual L	
	4	3.7	3.7	>2.5 (inc)	
RIBS	Mid-dorsal L	Post-dorsal L	Prox caudal L		
	18.8 (gentle curve: ~ 61° arc)	7.1 (~ straight)	7.3 (~ 90° bend)		
SACRAL RIB	Length	Prox Width	Mid-shaft W	Dist Width	
	5.8	2.4	1.5	5.2	

represented by six phalanges on block B with slightly concave proximal ends and trochlear distal ends. Two of these exhibit an unusual morphology of rounded proximal ends tapering sharply to a long, narrow shaft ending in a small trochlea, which we identify as penultimate phalanges with specialized articulating surfaces for the unguals. In addition to the partial ungual at the end of digit V, a single

complete ungual is preserved on block B. It is a laterally compressed, curved claw with a prominent flexor tubercle.

On block A, the left pes preserves five long, cylindrical phalanges similar to those of the right pes on block B, but all but one is broken and incomplete. Our reconstruction of the pes of *Eoscansor* (Fig. 10) is a composite based on the bones preserved on blocks A and B.

PHYLOGENETIC POSITION

The combination of a variety of features indicates that *Eoscansor* is a relatively primitive varanopid with an overlay of autapomorphies mostly related to its scansorial habitus. We note that Ford and Benson's (2020) recent claim that varanopids are not synapsids has already been challenged (Benoit et al. 2021), so we continue to regard varanopids as synapsids (eupelycosaurs).

There have been several published analyses of varanopid phylogeny, and these primarily employ cranial characters. Reisz (1986: 63), however, listed these features of varanopids that are present in *Eoscansor*: slender lower jaw; relatively short dorsal vertebrae; a low iliac blade with poorly developed dorsal trough; and fore- and hind limbs of nearly equal lengths and consist of relatively long, slender elements. Subsequent analyses identified as varanopid features a long and slender femur with an internal trochanter widely separated from the femoral head and set off from the proximal articular surface (shaft diameter 10% of femur length; it is 8.3% in *Eoscansor*) (Reisz and Modesto 2007) and a hind limb almost as long or longer than the trunk (Reisz et al. 2010). Reisz and Dilkes (2003) identified as varanopid autapomorphies a femur that is slender and long with a length-to-distal-width ratio greater than 3:1, and the possession of two subequal sacral ribs. All varanopids also have a slender dentary, short neural spines on dorsal vertebrae, and a mid-ventral ridge on all vertebrae according to Reisz and Dilkes (2003).

As Pelletier (2014) noted, phylogenetic analyses of eupelycosaurs are based primarily on cranial characters, which are 82–89% of the characters in the analyses of Anderson and Reisz (2004), Maddin et al. (2006), and Campione and Reisz (2010). Based primarily on the observations of Reisz and Dilkes (2003) and Reisz and Modesto (2007), Pelletier (2014) listed postcranial features characteristic of varanopids as: (1) mid-ventral margin of the dorsal centra ridged but without a distinct keel; (2) lateral excavation at bases of dorsal neural spines; (3) a plate-like head of the interclavicle; (4) two to three subequal sacral ribs; and (5) long and slender femur with a ratio of length to distal width greater than 3:1. We cannot evaluate feature 2 in *Eoscansor*, but it displays the other varanopid features listed by Pelletier (2014).

Pelletier (2014) also listed these features as synapomorphies of the more derived varanopids, the varanodontines: (1) tall neural spines; (2) double-headed ribs; (3) presence of a supraglenoid foramen; (4) broadly expanded proximal and distal ends of the humerus; (5) high degree of twist (torque) of the humeral heads about the shaft; (6) radius shorter than humerus; (7) expanded heads of the femur; (8) femur lacking sigmoid curvature; and (9) humerus and femur approximately subequal in length. *Eoscansor* shows most of these features, although the neural spines are only visible on the anterior cervicals, and the presence of a supraglenoid foramen cannot be determined.

An important point to make is that some of the indi-

vidual characters listed by Reisz (1986), Reisz and Dilkes (2003), and Pelletier (2014), as well as some other authors, as synapomorphies of Varanopidae occur in some other non-varanopid taxa. However, if those characters are judged collectively, as a whole, they are indicative of a varanopid relationship. Indeed, *Eoscansor* shows a combination of the characters considered to be synapomorphies of Varanopidae, and we recover it as a varanopid or as a sister taxon to Varanopidae in our phylogenetic analyses (see Appendices 1–3).

Benson (2012) included 147 cranial and 92 postcranial characters in a phylogenetic analysis of pelycosaurian-grade synapsids, and subsequent analyses have refined this dataset and incorporated new caseasaurian and varanopid taxa (Reisz and Fröbisch 2014; Brocklehurst et al. 2016; Maddin et al. 2020). Incorporating *Eoscansor* into the most recent of these analyses (Maddin et al. 2020) yielded 1,620 most parsimonious trees, each with 795 steps. *Eoscansor* is recovered as the sister taxon to *Archaeovenator hamiltonensis* in a clade diverging from the base of the Varanopidae (Fig. 11A, Appendix Fig. 1). This result is consistent with the relatively unspecialized dental anatomy and early appearance of both of these taxa.

In recent years, other workers have developed and refined independent datasets to investigate the phylogeny of varanopids (Spindler et al. 2018; Ford and Benson 2020). Each of these analyses incorporated a significant number of postcranial characters, but the majority of characters are derived from cranial anatomy that cannot be currently evaluated for *Eoscansor*. We attempted to analyze the relationships of *Eoscansor* using these datasets, but the results in each instance resulted in either unresolved polytomies or drastic modifications of the tree topology from that presented in the original analyses (Figs. 11B–C, Appendix Figs. 2–3). A summary of the characters we scored for *Eoscansor* in each of these datasets and the results of these analyses are presented in Appendix 2.

Spindler et al. (2018) noted that a clear understanding of the relationships of small varanopids was hampered by the incompleteness of fossil remains, a high potential for homoplasy, and poorly understood character histories among Paleozoic amniotes. It is likely that each of these issues impacted the results of the analyses when *Eoscansor* was included, underscoring the challenges in determining the relationships of Paleozoic amniotes lacking cranial material.

Finally, we did consider the possibility that *Eoscansor* is a diapsid, as some of the early diapsids are small, slenderly built tetrapods. However, if we compare *Eoscansor* to the basal diapsids *Petrolacosaurus*, a near contemporary, and the slightly younger (early Permian) *Araeoscelis*, they have several postcranial synapomorphies not seen in *Eoscansor*, such as elongated cervical vertebrae (and thus a long neck); swollen neural arches with deep lateral excavations on the cervical, dorsal, and sacral vertebrae; limb bones with very slender proximal and distal ends; radius nearly equal in length to humerus; and tibia nearly equal in length (Reisz 1981; Reisz et al. 1984).

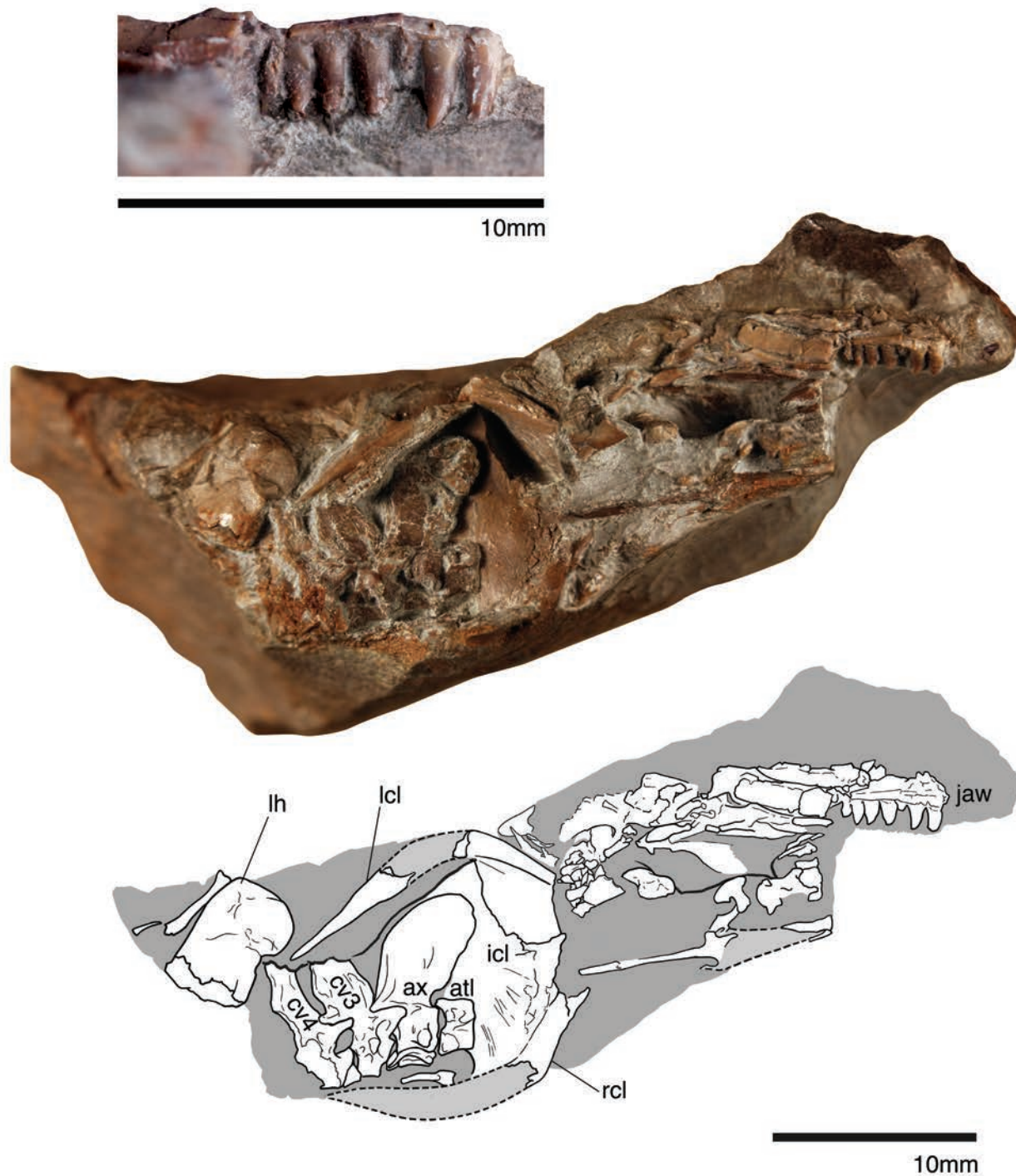


Fig. 7.—Photograph of dentition (above), and photograph (middle) and bone map (below) of NMMNH 75122, holotype of *Eoscansor cobrensis*, the block containing a lower jaw fragment and other bones. Abbreviations are: atl = atlas, ax = axis, cv = cervical vertebra, icl = interclavicle, lcl = left clavicle, lh = left humerus, rcl = right clavicle.

SIZE

Before discussing the anatomical features of *Eoscansor* that indicate it was scansorial, we estimated its weight (mass), tail length, and overall length.

Mass

Several workers have produced scaling equations to relate limb bone metrics to body mass in mammals, birds, dinosaurs, and generalized tetrapods (e.g., Anderson et al. 1985; Christiansen 1999; Campione and Evans 2012). Christiansen's (1999) work is specific to mammals, so we used the scaling equations of Anderson et al. (1985) and Campione and Evans (2012). In both methods the sum of the midshaft circumferences of the humerus and femur are required to estimate mass. In *Eoscansor*, the femur is essentially round in cross section, with a diameter of 1.85 mm and circumference of 5.81 mm. The humerus has a minor diameter of 1.63 mm, a major diameter of 1.78 mm, and a circumference of 5.36 mm. The sum of the circumferences, $C_{H+F} = 11.17$ mm.

The body mass (BM) scaling equation of Anderson et al. (1985), $BM = 0.078 \cdot C_{H+F}^{2.73}$ yields a body mass of *Eoscansor* of 56.7 g. Solving the scaling equation of Campione and Evans (2012), $\log BM = 2.749 \cdot \log C_{H+F} - 1.104$ (base 10 logs are used), yields a body mass of 59.9 g.

Thus, the two methods agree to within approximately 5%. Averaging the two results gives us a mass estimate for *Eoscansor* of 58.3 g.

We compare the calculated mass (as \log_{10} g) and SVL (as \log_{10} mm) of *Eoscansor* to those of several hundred extant lizard species after Meiri (2010: fig. 1) (Fig. 12A). In the plot, legless and reduced-limb species are excluded. "Crosshairs" show the position of *Eoscansor* at 125 mm SVL and 58.3 g mass. The mass of lizards of similar SVL to *Eoscansor*, along the vertical 125 mm SVL line, varies from 16 g to 100 g. Thus, *Eoscansor* falls at approximately 50% of the range of masses for its SVL and is shown to be of average build for its SVL.

Tail Length

The tail length of *Eoscansor* was estimated by first determining the taper of the preserved portion of the tail (Fig. 13A) and then calculating the necessary length at that taper for the tail to reach the point of zero width (Fig. 13B). Assumptions here are that the tail taper is constant from base to tip and that the tip is pointed.

A trigonometric method, as used by Landman et al. (2004: fig. 16) to calculate the taper of baculites (heteromorph cephalopods), was used here to calculate the tail taper of *Eoscansor*: Taper = $2 \cdot \text{ATAN}((\text{Width 2}-\text{Width 1})/\text{Length})$

Where Width 2 is the width of the basal caudal vertebra

(3.13 mm in *Eoscansor*), Width 1 is the width of caudal ~10 (2.57 mm), and Length is the distance from the basal caudal to caudal 10 (42 mm) (Fig. 11A). Because the caudal series is incomplete, this estimate is based on impressions as well as preserved vertebrae. The resulting tail taper for *Eoscansor* is 1.5°.

In order to calculate the tail length, it was assumed to be a right triangle in longitudinal section (Fig. 13B) wherein the angle, C, is 90°. Although the tail is actually an isosceles triangle, the assumption of a right triangle simplified the calculation without introducing a significant error. This is because the tail represents a very elongate triangle in which the exact tail length, side AC of the triangle, is essentially identical to side AB, which is easily calculated (Fig. 13B). The tail length is then: $AC \approx AB = BC/\sin 1.5^\circ$ where BC is the width of the basal caudal vertebra and 1.5° is the tail taper. The resulting tail length is 120 mm.

Total Length of *Eoscansor*

A straightforward measurement of the fossil yields an SVL of 125 mm. Together with the tail length calculation of ~120 mm, we estimate the overall length of *Eoscansor* to be 245 mm.

Scansorial adaptations of *Eoscansor*

Here, we discuss several scansorial adaptations that are present in *Eoscansor* and compare them with those of more ground-oriented varanopids and some other taxa, notably extant lizards. These adaptations are best understood in terms of forelimb and hind limb anatomy and other aspects of the skeletal anatomy of *Eoscansor* (Fig. 14). Many of these adaptations show up in the metric ratios of various body segments or bones, and appropriate data to make these comparisons are sometimes difficult to obtain. For example, large tables of important eupelycosaur bone measurements are available in Romer and Price (1940), but it is not possible to associate the specific bones of one individual with certainty. Comprehensive measurements are available for *Aerosaurus*, including the holotype, in Langston and Reisz (1981), where it is possible to know that the various measurements all belong to the same individual. Thus, generalized comparisons are made to *Varanosaurus* and *Varanops*, but where metrics are required, we use *Aerosaurus* or extant lizards. Here, we review the anatomical evidence that supports scansoriality by *Eoscansor* from the strongest to the weakest evidence, beginning with a brief discussion of its overall features among climbing tetrapods.

Bauplan

Hildebrand and Goslow (2001) made an important distinction between scansorial, which means climbing, and arboreal, which means living in trees. Thus, many birds are

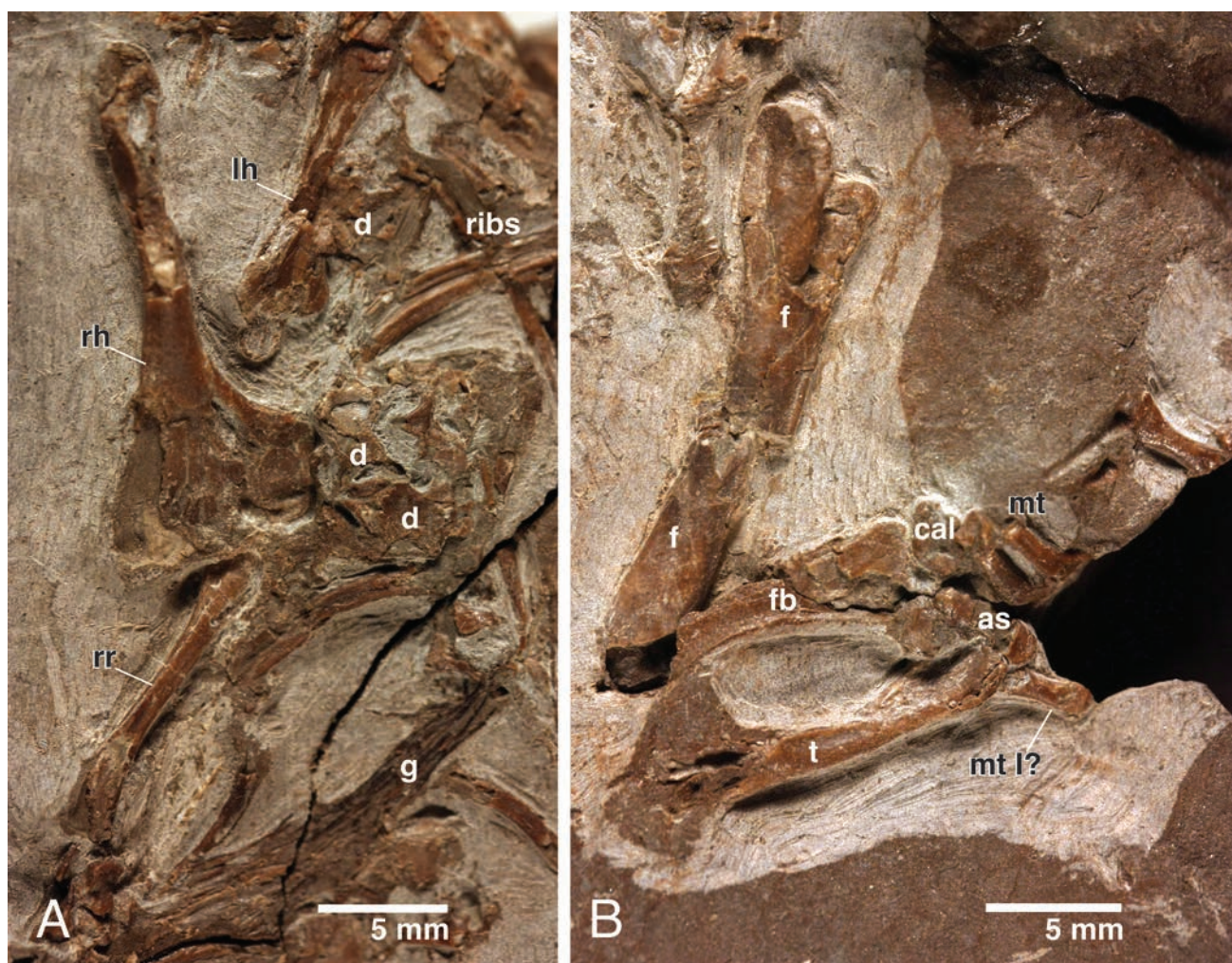


Fig. 8.—Photographs of selected enlarged portions of NMMNH P-75122, holotype of *Eoscansor cobrensis*. **A**, right humerus and associated bones on block A. **B**, part of hind limb on block B. Abbreviations: as = astragalus, ca = calcaneum, d = dorsal vertebra f = femur, fb = fibula, g = gastralia, lh = left humerus, mt = metatarsal, rh = right humerus t = tibia. Scale bars = 5 mm.

arboreal (live in trees) but they do not climb in trees (they are not scansorial). Tetrapods undertake tree climbing to secure food, find shelter, escape predation, or have freedom of movement when ground vegetation is dense. All major groups of tetrapods have scansorial members. Indeed, today there are amphibians, reptiles, mammals, and birds that are scansorial, and the range of scansorial adaptations of tetrapods is broad. Thus, there is a wide range of scansorial adaptations and body plans, so we have limited our consideration of scansors comparable to *Eoscansor* to those that can be described as small, nonacrobatic climbers, which is the mode of scansoriality we posit for *Eoscansor*. Nevertheless, Jenkins (1974) showed that the morphological adaptations of small animals that clamber over uneven, littered ground are not very different from those that climb rocks or trees, and that a small animal that runs along large tree branches is not very different from

an open ground runner. This provides a note of caution to our analysis by forcing us to focus on unequivocal anatomical correlates of scansoriality in *Eoscansor*. Here, we characterize small, nonacrobatic climbers based primarily on the observations and analyses of Cartmill (1974, 1985) and Hildebrand and Goslow (2001).

Branches and tree trunks differ from the earth's surface in four important ways—they are discontinuous, limited and variable in width, mobile, and oriented at various angles with respect to gravity (Cartmill 1985). Thus, climbing requires propulsion on discontinuous and three-dimensional substrates without falling. Claws are superior to both pads and nails when climbing vertical trunks or branches. Many climbers have sharp claws that are recurved at their tips, and they climb by interlocking, which is inserting the claws into cracks or crevices in the substrate to grip. Small, nonacrobatic climbers tend to have

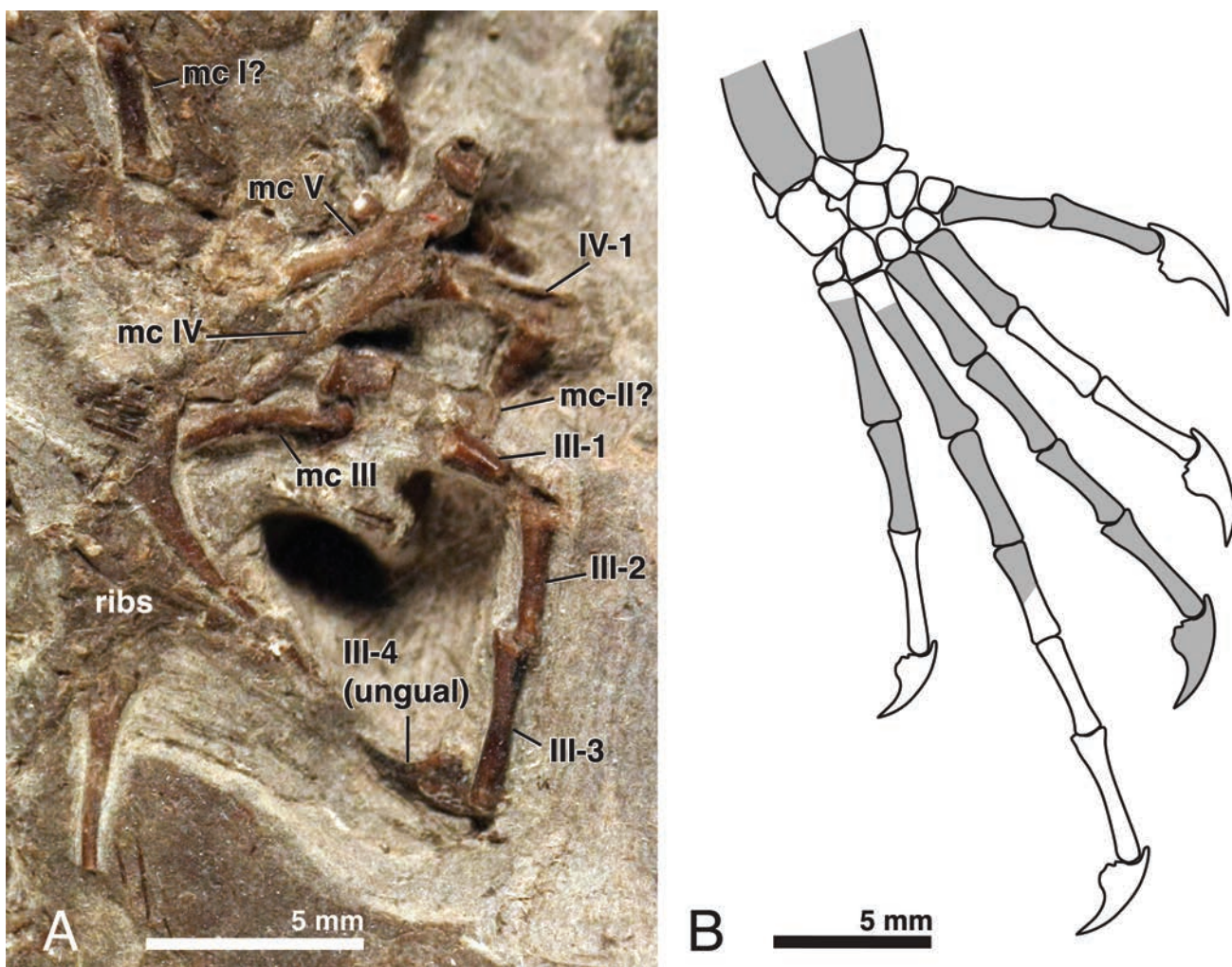


Fig. 9. — Manus of NMMNH P-75122 on block B, holotype of *Eoscansor cobrensis*. A, photograph of better preserved manus. B, reconstruction of the bones of the manus. Abbreviations; mc = metacarpal; II, III and IV = digit number. Missing bones (not shaded) based on *Ascendonanus*. Scale bar = 5 mm.

an elongate trunk in which the thorax contributes disproportionately to total trunk length, and forelimbs are nearly equal in length to the hind limbs. The goal is to keep the center of gravity low. Legs are generally short, and the tail is long.

Cartmill (1974, 1985) and Hildebrand and Goslow (2001) provided useful overviews of the osteological correlates of climbing in vertebrates that allow some generalizations to be made. Key to climbing is the ability to interlock by cutting sharp claws into cracks and/or crevices in an inclined arboreal substrate for support. Flexibility and agility are key features of climbers, and marked strength is not needed, so robust muscle attachments are absent. Many adept climbers propel themselves by reaching upward, pulling along, or bridging. Thus, they have long reach with proximal and middle limb segments of nearly equal length, a long thorax, and large, gripping feet.

The heads of the humerus and the femur are hemispherical (nearly complete spheres), the ulna and radius are free and about equally developed, the proximal head of the radius is round, the radial notch is evenly curved and lateral in position, and the styloid process at the distal end of the ulna forms a pivot around which the carpus turns. The patellar groove is shallow, and the greater trochanter is small. The fibula is free and relatively large with an ellipsoidal, not a hinge-like joint with the tarsus so that rotation, abduction, and adduction of the tarsus are facilitated. The hemispherical humeral head is for well-developed shoulder mobility (no substantial trochlea to interfere). Digits are subequal in length.

Limb bones are lightly built and slender without large muscle attachments. The levers of the extensor muscles are relatively short, and better developed are the flexors, pronators, supinators, and abductors. Digital flexors are well

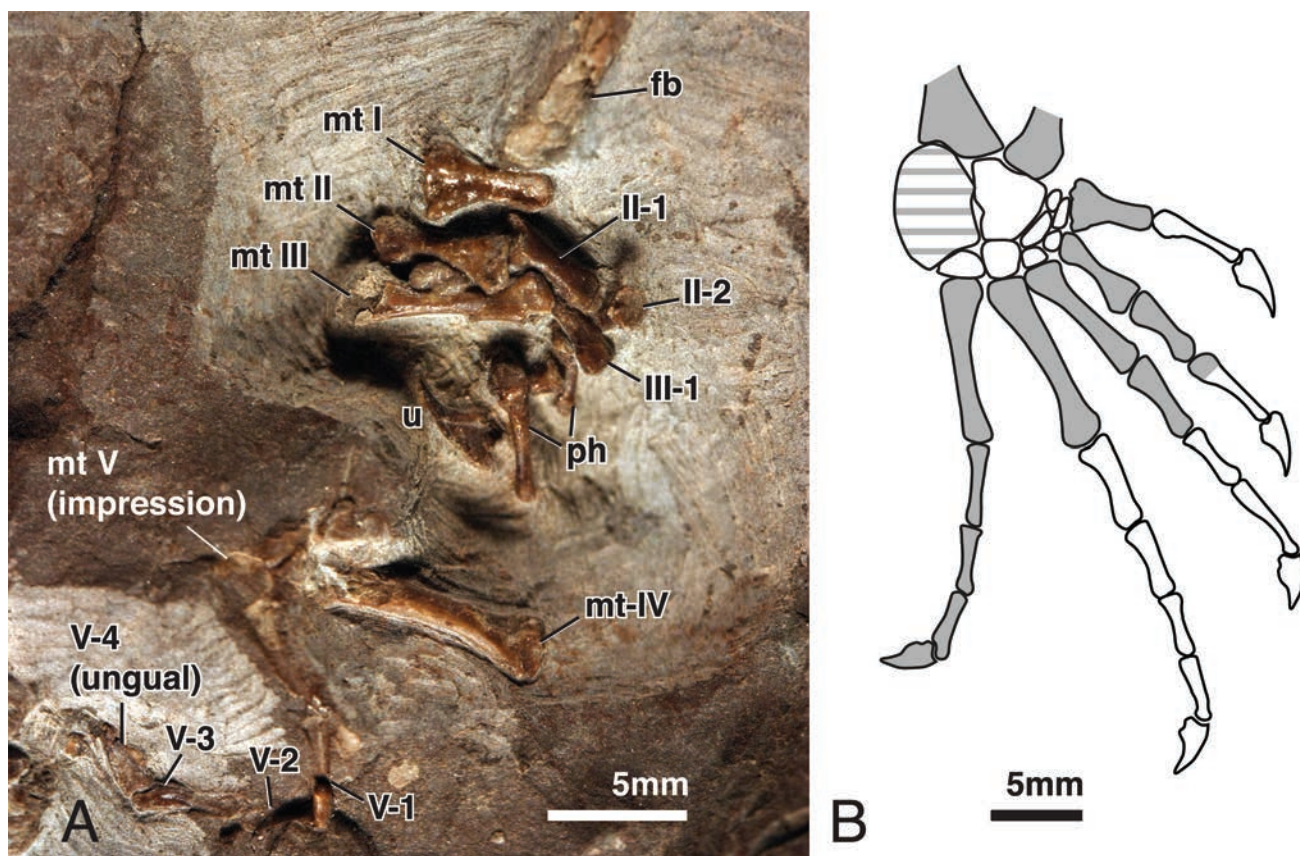


Fig. 10.—Pes of NMMNH P-75122 on block B, holotype of *Eoscansor cobrensis*. A, photograph of better preserved pes. B, reconstruction of the bones of the pes. Abbreviations: fb = fibula, mt = metatarsal; ph = phalanx, un = ungual phalanx, II, III, IV and V = digit number. Bones that are preserved in *E. cobrensis* are shaded. Missing bones (not shaded) based on *Ascendonanus*. Scale bar = 5 mm.

developed for grasping to resist slipping. Some climbers have an opposable digit I and a prehensile tail that is long, ventrally curved, and flexible at the base. Structural modification of the hallux to permit it to move independently produces hallucal prehensility for climbing (Jenkins and Parrington 1976).

In spite of difficulties caused by ecological and size-related factors, several workers have made advances toward finding biometric evidence of behaviors such as climbing, arboreality, open ground running, etc., in specific tetrapods (e.g., Vanhooydonck and Van Damme 2001; Zaaf and Van Damme 2001). Here, we rely on such analyses when evaluating the scansoriality of *Eoscansor*.

Claws

Both the manual and pedal claws of *Eoscansor* are long, sharply pointed, strongly curved, laterally compressed, and have pronounced flexor tubercles (Fig. 15). This particular claw morphology, especially the strong curvature, has long been recognized as a characteristic of scansorial tetrapods. Note that we consider that the ungual phalanges of *Eoscansor* correctly reflect the fully sheathed claw cur-

vature and are thus able to be used to predict habits, as has been accepted practice in paleontology since the work of Feduccia (1993) (e.g., Spielmann et al. 2006; Fröbisch and Reisz 2009, 2011; Spindler 2018, and others).

The proximal ends of the claws of *Eoscansor* have a robust, well-defined surface to receive the articular surface of the distal penultimate phalanx to form a ginglymus that restricts motion at the joint to the parasagittal plane. The pedal claws are slightly larger in their dorsoventral dimensions and probably experienced greater dorsoventral stress than the manual claws, but are of the same basic geometry. The scansorial adaptations of *Eoscansor* claws are: (1) strong claw curvature; (2) manual and pedal claws show same curvature; and (3) large flexor tubercles.

Claw curvature—We measured the claw curvature of *Eoscansor* by applying a geometric method devised by Feduccia (1993) that uses highly enlarged photographs of the manual and pedal claws in lateral view (Fig. 15). First, the area over which the arc of curvature was to be measured was spanned by line AB (Fig. 15A). Line AB was then bisected by line CD, and the point where CD meets the ventral edge of the claw arc was labeled X so that a

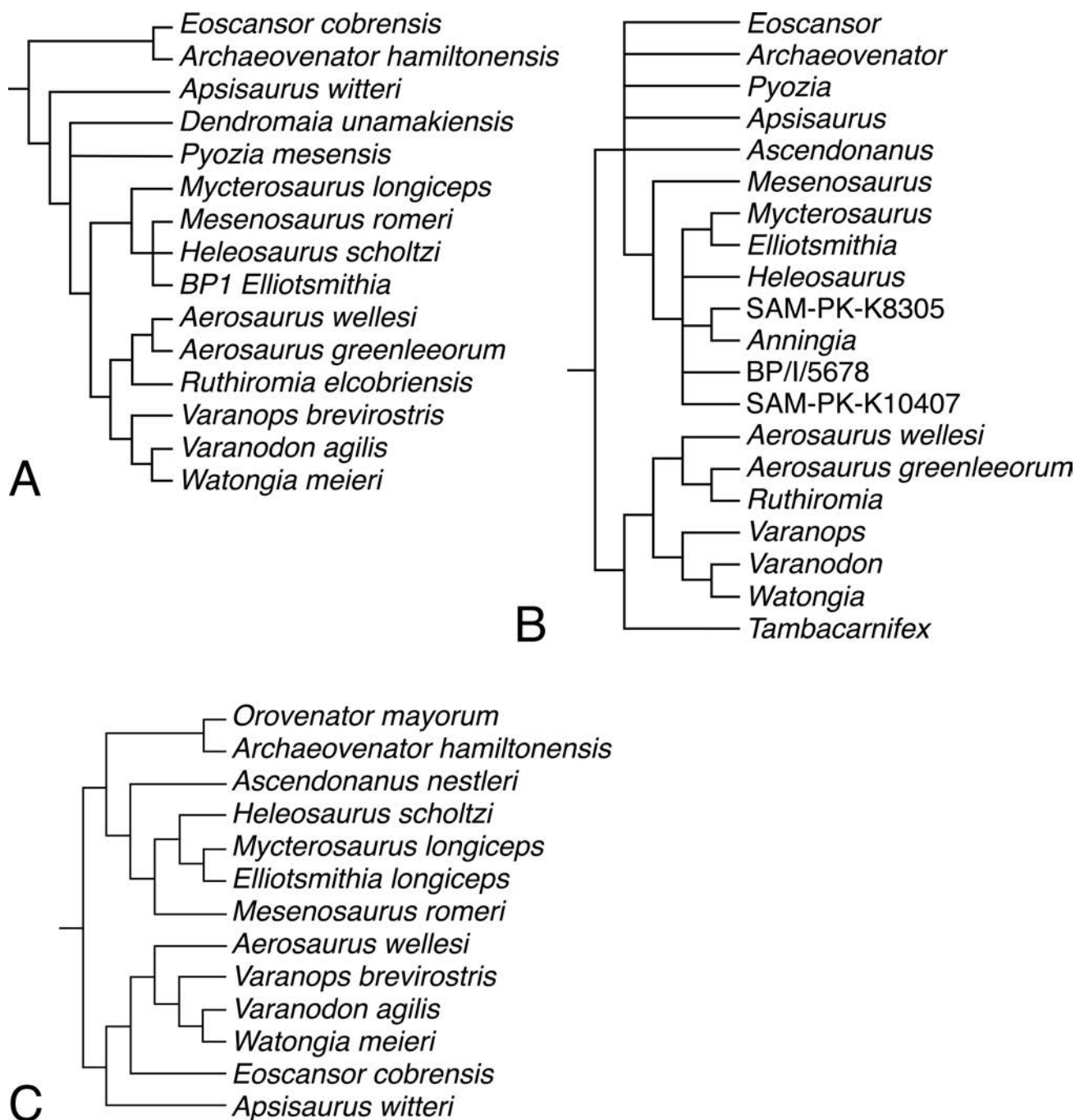


Fig. 11.—Phylogenetic position of *Eoscansor* in three recent phylogenetic hypotheses of varanopid relationships. A, Maddin et al. (2020). B, Spindler et al. (2020). C, Ford and Benson (2020). See the text and Appendix B for discussion and analysis.

triangle, ABX, was constructed. Next, sides AX and BX of the triangle ABX were bisected by lines EE' and E'E''. These two lines were extended until they met under the center of the claw arc at point E'. Finally, lines AE' and BE' were constructed, forming triangle ABE'. The angle E', which equals the claw curvature, was measured using

a protractor. The resulting claw curvatures for *Eoscansor* are 91.5° for the manual claw and 92° for the pedal claw – both of which are strongly curved at essentially 92°.

Comparative claw curvatures—Differences in claw curvature have been well correlated with ground-dwelling

TABLE 2. Claw curvature arc in various species. References: 1, Mann et al. (2021); note: Mann et al. (2021) did not specify whether manual or pedal claw curvature was measured; 2, Feduccia (1993); 3, Spielmann et al. (2008: fig. 124); 4, author's measurements using Feduccia's (1993) method based on Fröbisch and Reisz (2011: figs. 9 [manus] and 13C [pes]); 5, author's measurements using Feduccia's (1993) method based on Spindler et al. (2018: fig. 29); 6, Spindler et al. (2018), measuring the arc of the dorsal edge of the claws rather than the ventral edge as in the Feduccia (1993) method; 7, author's measurements based on Spielmann et al. (2008: fig. 115), originally from Renesto and Paganoni (1995); 8, Spielmann et al. (2006: fig. 3).

Taxon	manus	pes	reference
<i>Anthracodromeus</i>	97°	97°	1
<i>Archaeopteryx</i>	147°	120°	2
<i>Trilophosaurus</i>	142°	117°	3
<i>Suminia</i>	102°	108°	4
<i>Ascendoranatus</i>	~118°	~118°	5
<i>Ascendoranatus</i>	115°–171°	115°–171° pedal?	6
<i>Sciurus</i> (squirrel)	109°		7
<i>Coelophysis bauri</i>	153°	39°	This study
<i>Drepanosaurus</i>	~75°–95°	57°–95°	8
<i>Megalancosaurus</i>	~80°–91°	50°–90°	8
<i>Vallesaurus</i>	95°–100°	86°–110°	8
<i>Eoscansor</i>	92°	92°	This study

and climbing habits in various vertebrate species (e.g., Hildebrand and Goslow 2001: fig. 26.12 and associated text). Zani (2000) showed a positive correlation between increasing claw curvature and clinging performance on rock and wood surfaces, and Spielmann et al. (2006) demonstrated claw curvature to be important in assessing scansoriality in Late Triassic drepanosaurids. Scansorial mammals also have similar ungual claws characterized by high curvature (e.g., Krause and Jenkins 1983; Cartmill 1985; Van Valkenburgh 1987; Rose 1990; Kielan-Jaworowska and Gambaryan 1994).

Feduccia (1993: fig. 2–3) used claw curvature to diagnose arboreal habits in the Late Jurassic bird *Archaeopteryx*. He showed that the overall distribution of bird claw curvatures consists of three component distributions that represent ground dwellers, perchers, and climbers. In addition to other factors, Spielmann et al. (2005, 2008), Fröbisch and Reisz (2009, 2011), and Spindler et al. (2018) used claw curvature in the Late Triassic archosauromorph *Trilophosaurus*, the late Permian anomodont synapsid *Suminia*, and the early Permian varanopid eupelycosaur *Ascendoranatus*, respectively, as evidence of climbing behavior. Three genera of Late Triassic drepanosaurids show less claw curvature than the above-mentioned reptiles, but they are nonetheless considered scansorial (Spielmann et al. 2006) (Table 2).

In the late Permian scansorial anomodont synapsid *Suminia*, manual claws were measured using the methodology demonstrated in figure 9 of Fröbisch and Reisz (2011, digit 3 or 4) per Feduccia (1993) to subtend 102° of cur-

vature. The pes claws measured 108° of curvature using figure 13C of Fröbisch and Reisz (2011, digit 3) (Table 2). Both *Suminia* and *Eoscansor* claw curvatures are well above Feduccia's (1993) ground-dwelling range of means for bird species (52.2° to 77.6°, overall mean = 64.3°), and both are well below his trunk-climbers range of means for bird species (129.5° to 161.6°, overall mean = 148.7°). Species of perching birds show a range of means of 101.8° to 125.3° (overall mean = 116.3°). The claw curvatures of *Eoscansor* occupy the morphospace just below the perching birds, and *Suminia* claw curvatures are within the lower portion of values for perchers (Feduccia 1993: fig. 3). Yet, neither *Suminia* nor *Eoscansor* are birds. Certainly, some animals that are accomplished tree climbers do not show the high claw curvatures of trunk-climbing birds. For example, the squirrel claw illustrated by Renesto and Paganoni (1995) measures 109° curvature, placing it within the lower part of the perching birds (Feduccia 1993: fig. 3), similar to *Suminia* and *Eoscansor*.

Suminia claws have 10 to 16° more curvature than *Eoscansor*, which is a small amount on a scale that extends up to ~162° for birds (Feduccia 1993) and at least up to 155° for climbing reptiles (Spielmann et al. 2008). Additionally, the claw curvatures of *Eoscansor* fall well within the range of the arboreal drepanosaurids *Drepanosaurus*, *Megalancosaurus*, and *Vallesaurus* (Table 2). The claw curvature of *Eoscansor* thus places it within the established range for climbing reptiles.

As pointed out by one of our reviewers, living *Chamaeleon* is an example of a grasping animal with straight

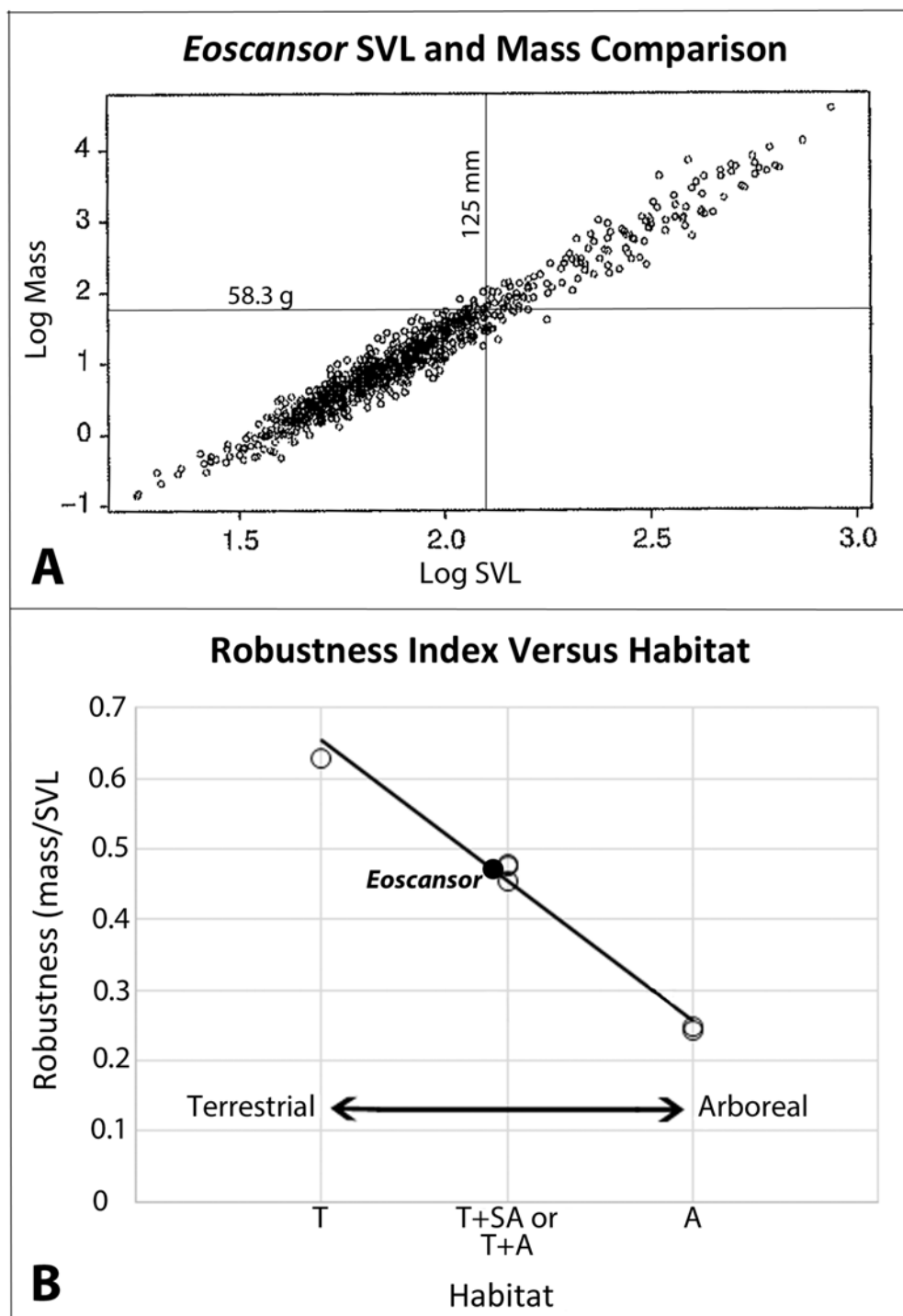


Fig. 12.—*Eoscansor* mass and SVL. A, comparison of mass and SVL of *Eoscansor* to those of ~900 lizard species spanning 33 families (after Meiri 2010). Crosshairs show the location of *Eoscansor* on the plot. Axes are \log_{10} . B, relative robustness (mass/SVL) of six extant lizards of similar SVL to *Eoscansor*. In terms of robustness, *Eoscansor* groups best with the species that have both terrestrial and arboreal habits. Fully terrestrial animals are more robust, fully arboreal animals are more gracile. Habitat definitions: T = terrestrial, T+SA = terrestrial plus semi-arboreal, T+A = terrestrial plus arboreal, A = arboreal.

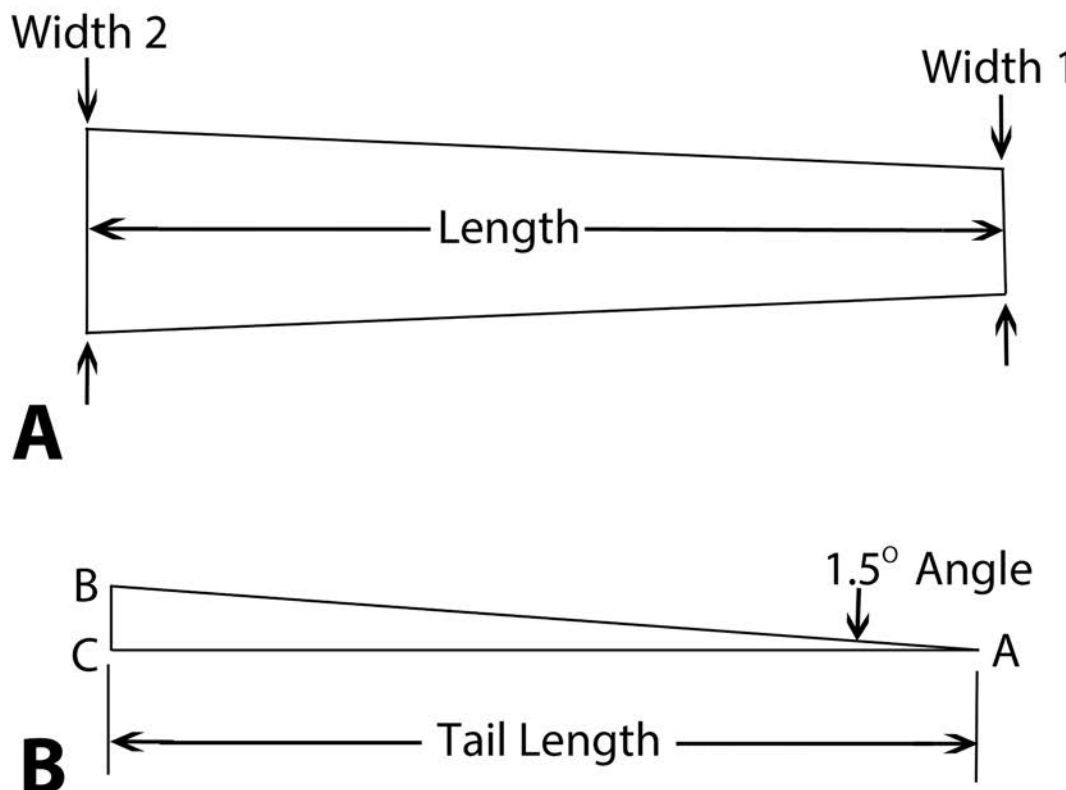


Fig. 13.—Tail length. Geometric representations used in the tail taper and length calculations. **A**, a segment of the proximal tail. Width 2 equals the basal tail width; Width 1 equals the tail width at the end of the segment over which taper is calculated, and Length equals the segment length. **B**, the tail in longitudinal section approximated as a right triangle ABC, where angle A equals the tail taper of 1.5° ($\sim 5^\circ$ in the figure for clarity), BC equals basal tail width, and BA equals tail length.

claws, so not all climbers have curved claws. However, we note that *Chameleon* is a unique and very highly derived taxon with a generally coiled, prehensile tail, unusual skeletal and skull characters, an almost ceratopsian-like neck shield, a highly arched back, and hands and feet that feature extreme divergence of the digits similar to those of zygodactylous birds. Additionally, *Chameleon* hunts using stealth and its projectile tongue, not by running or jumping and capturing prey in its mouth as most lizards do. It seems to us that the short and strait claws of *Chameleon* have little relevance to a tetrapod such as *Eoscaenior*, which has a much more “conventional” lizard bauplan. Perhaps if a varanid or lacertid with short, straight claws and a body plan similar to *Eoscaenior* could be found it would make this argument more valid. The highly derived *Chameleon*, we would argue, is not a good functional analogue of *Eoscaenior*.

Similar curvature of manual and pedal claws—In climbers, the manual and pedal claws are typically the same curvature because they engage the substrate (through interlocking) and support the weight of the animal in the

same way. The same is true of ground-oriented animals—where the manual and pedal claws have similar curvatures but are much less than those of climbers.

In *Eoscaenior*, the geometry in general and the curvature in particular of both the manual and pedal claws is essentially identical (92°). This places it in the range of climbing reptiles and mammals and indicates that the claws of both the hands and feet served a similar function. Thus, the similar high curvature of manual and pedal claws of *Eoscaenior* indicate that both its hands and feet were adapted to a single purpose, that of climbing.

By comparison, the claw curvature of the more ground-oriented varanopid *Aerosaurus* is between 25° and 37° as measured from the illustrations of the holotype by Peltier (2014). The manual and pedal claws of *Varanosaurus* show similar curvature to those of *Aerosaurus* and are not considered to be within the range of climbers (see illustrations of Campione and Reisz 2010). The claws of *Anthracodromeus* are unusual in that they show a high degree of inner curvature just distal to the region where the flexor tubercle would be located. Although *Anthracodromeus* lacks

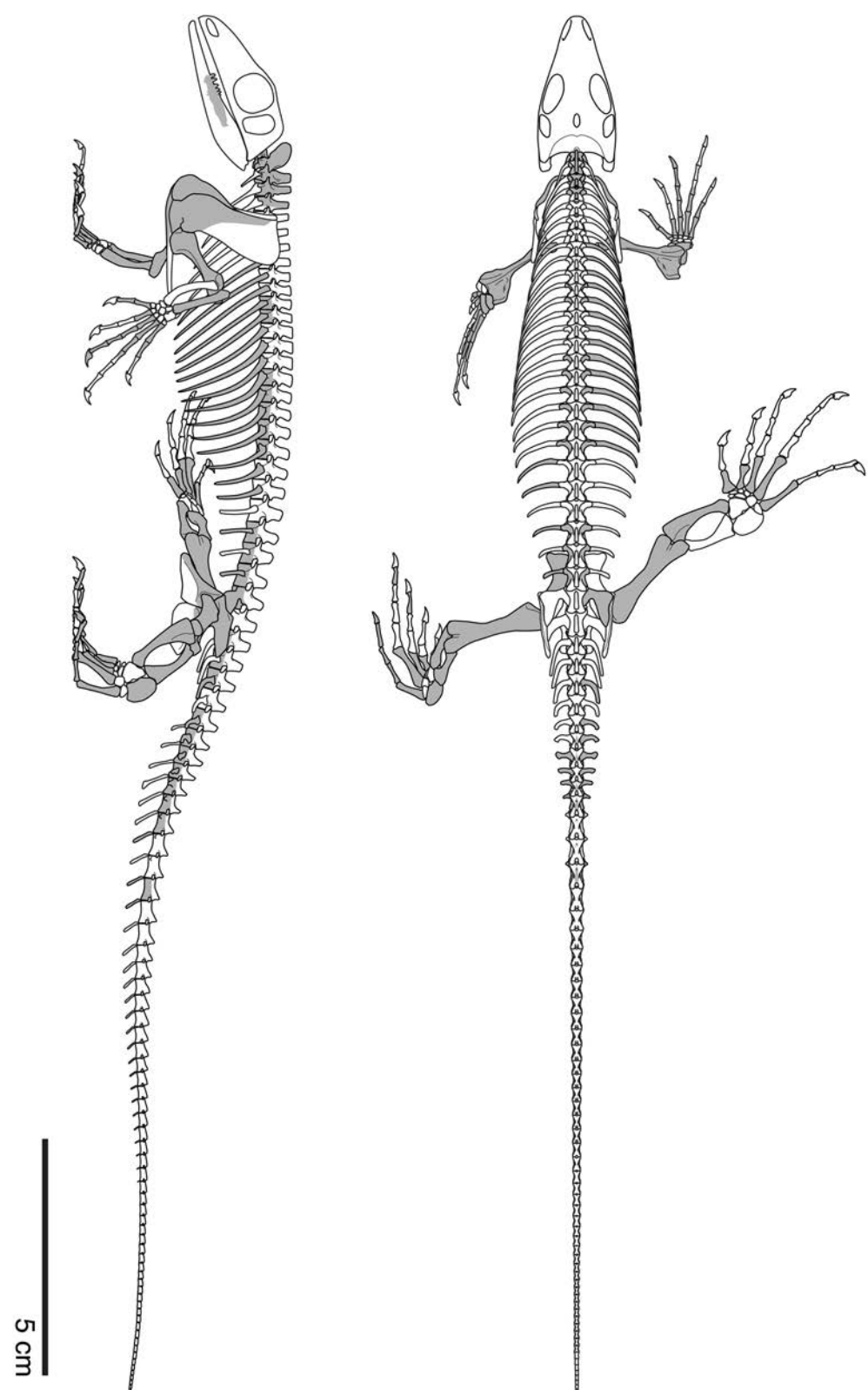


Fig. 14.—Reconstructed skeleton of *Eoscaenor* in dorsal (above) and left lateral (below) views. Skull based on the skull of *Mycterosaurus*. Scale bar = 5 cm.

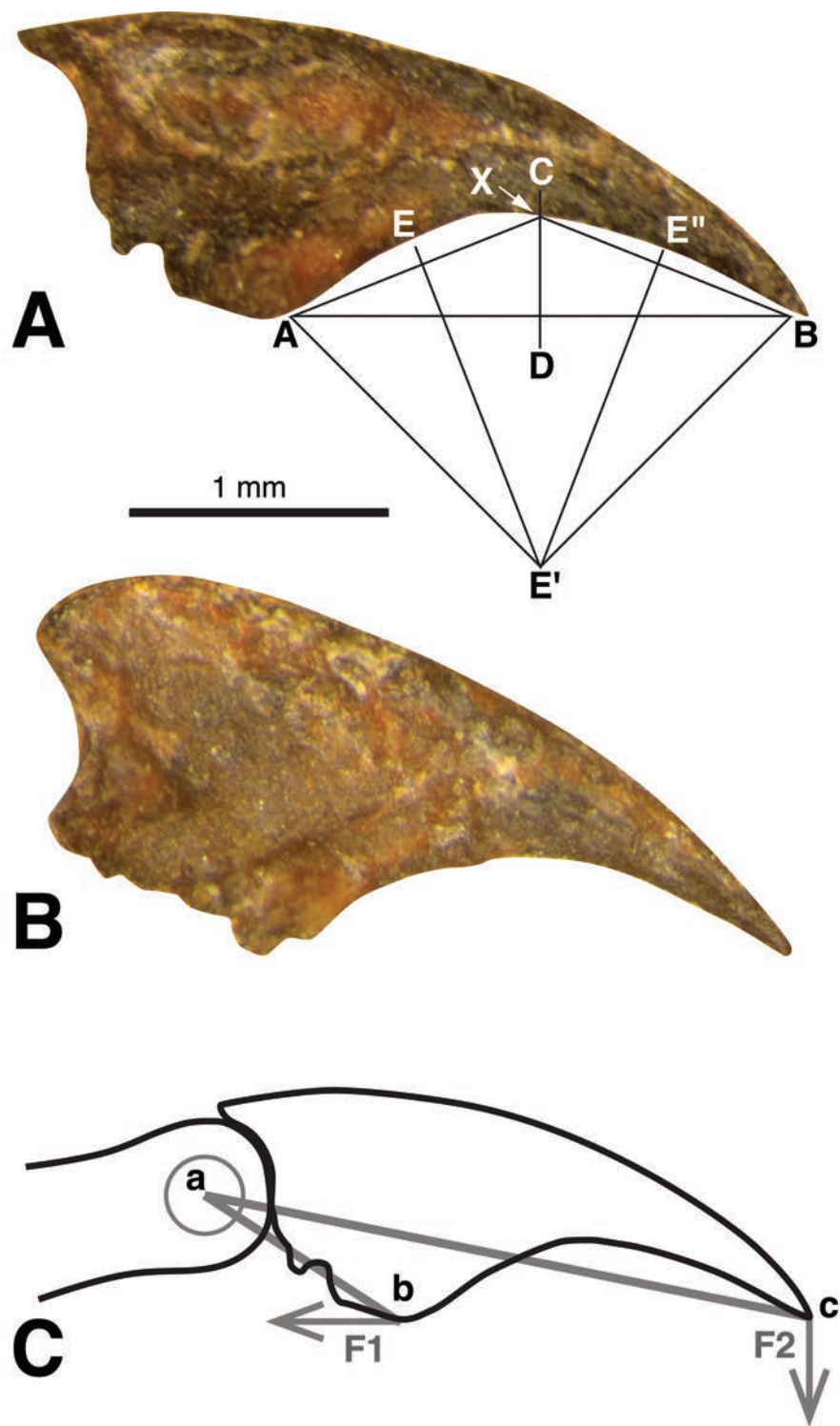


Fig. 15—Claws of *Eoscansor* in lateral view. A, manual claw with construction lines for determining claw curvature (per Feduccia, 1993, see text). B, pedal claw with incomplete flexor tubercle. C, schematic of the manual claw with distal penultimate phalanx. Axis of claw rotation is at point a. Line ab represents the lever arm for the digit flexor. Force F1 is applied to the flexor tubercle by the digit flexor and force F2 is applied to the substrate. After Hildebrand and Goslow (2001: fig. 26.12).

a flexor tubercle, the distal phalanx (claw) is composed of an essentially straight section comprising about half of the claw length, and, finally, a sharply hooked curvature near the distal tip (Mann et al. 2021: supplemental material, fig. S6). The extra length of the claws introduced by the “straight section” works against the mechanical advantage of the digit flexor and would reduce the force applied to the substrate by the claw tip (F2 in Fig. 15). However, their overall inner curvature of 97° does place them within the range of scanners.

When the hands and feet are adapted for different purposes, the manual and pedal claws can be of radically different geometries. For example, the Late Triassic theropod dinosaur *Coelophysis* shows radically different curvatures in its pedal claws, which are those of a cursorial biped, and its manual claws, which were adapted for grasping and grappling with prey (Rinehart et al. 2009). *Coelophysis* manual claws (NMMNH specimen P-42353) measure 153°, similar to those of climbing birds and reptiles, and its pedal claws (NMMNH specimen P-42200) measure 39°, similar to those of the ground-dwelling varanopids *Aerosaurus* and *Varanosaurus*.

Flexor tubercles—The claws of *Eoscansor* have large, well-defined flexor tubercles that comprise about 40% of the proximal claw height (Fig. 15). In part, the flexor tubercle height determines the leverage provided to the digit flexor muscles that rotate the claw tip as it engages the substrate (Hildebrand and Goslow 2001). In a schematic representation of the lever system (Fig. 15C) line ab, the length of the lever arm, extends from the axis of rotation, centered in the rounded terminus of the penultimate phalanx, to the apex of the flexor tubercle. As the flexor tubercle becomes larger, line ab becomes a proportionately longer lever, so that more of the force applied by the digit flexor muscles (F1) is transferred to the substrate (F2). Other factors that influence the effectiveness of the lever system include the claw length and the angle between the applied force (F1) and the lever arm (ab), which changes throughout the rotation of the claw. Thus, the large flexor tubercles of *Eoscansor* provided an increased mechanical advantage for rotating the claw to engage the substrate for grasping and/or climbing.

The flexor tubercles of both *Aerosaurus* and *Varanosaurus* (illustrations by Pelletier (2014) and Campione and Reisz (2010), respectively) are poorly developed and comprise less than 10% of overall proximal claw height, as is common in nonclimbing tetrapods (Hildebrand and Goslow 2001: fig. 26.12 and associated text). These small flexor tubercles provided much less mechanical advantage to the digit flexor muscles than did those of *Eoscansor*. As previously discussed above, flexor tubercles are absent in *Anthracodromeus*.

Non-ungual Phalanges and Metapodials

The non-ungual phalanges and metapodials of *Eoscansor* also have morphological features that are adaptations for

climbing: (1) elongate proximal and penultimate phalanges; (2) high phalangeal index (of Fröbisch and Reisz 2009); and (3) metapodial of digit I relatively short with wide proximal end.

Elongate proximal and penultimate phalanges. Fröbisch and Reisz (2009) noted that often in the grasping hands and feet of scansorial tetrapods the proximal phalanges are relatively elongated. This adaptation occurs in animals as diverse as lizards, some Mesozoic mammals, marsupials, primates, carnivorans, and rodents (e.g., Luo et al. 2003; Kirk et al. 2008; Zheng et al. 2013). The possession of elongated penultimate phalanges is an indicator of clinging and/or arboreal ability (also see Hopson 2001). In *Suminia* both the proximal and penultimate phalanges are elongated, and the intermediate phalanges are reduced to short, tablet-like discs. This condition was used to indicate grasping and clinging ability, and general arboreality in this therapsid (Fröbisch and Reisz 2009). Using principal components analysis and character correlation studies, Fontanarrosa and Abdala (2016) also noted that the presence of elongate proximal and penultimate phalanges in the hands of lizards correlates with grasping capabilities and is a general indicator of arboreality.

In *Eoscansor*, the proximal and penultimate phalanges are longer than the intervening phalanges (Table 1; Figs. 9–10, 14). Unlike *Suminia*, however, in *Eoscansor* the intermediate phalanges are not reduced to discs, but are simply similar in appearance, though shorter. The phalangeal proportions of *Eoscansor* are much like those of the scansorial lacertid lizard *Holaspis* (e.g., Fröbisch and Reisz 2009: fig. 4e). Thus, the elongate proximal and penultimate phalanges in *Eoscansor* are an adaptation for grasping and clinging, and we believe them to be strong indicators of scansorial behavior. Additionally, they bear significantly on the phalangeal index as discussed below.

Phalangeal index—As mentioned above, Fröbisch and Reisz (2009) noted that among the arboreal tetrapods the hands and feet often showed specialization in the form of the elongation of the proximal and penultimate phalanges. From these observations, they developed a “phalangeal index” (PI), which is the sum of the proximal and penultimate phalangeal lengths expressed as a percentage of the length of their associated metapodial:

$$\text{PI} = (\text{L}_{\text{metapodial}} / (\text{L}_{\text{prox phalanx}} + \text{L}_{\text{penultimate phalanx}})) \cdot 100$$

In the manus of *Eoscansor*, the proximal and penultimate phalanges of the third digit are 3.9 mm and 4.1 mm long, respectively, and their associated metacarpal is 3.95 mm long, which yield a phalangeal index of 202%. In the pes, the lengths of the proximal and penultimate phalanges of digit 5 and their associated metatarsal measure 4 mm, 3.7 mm, and 8.6 mm, respectively. The resulting phalangeal index for the pes is 117%. These high (>100%) phalangeal indices strongly indicate scansorial capability.

For comparison, we used the illustration of Langston and Reisz (1981: fig. 16) to calculate the phalangeal indices

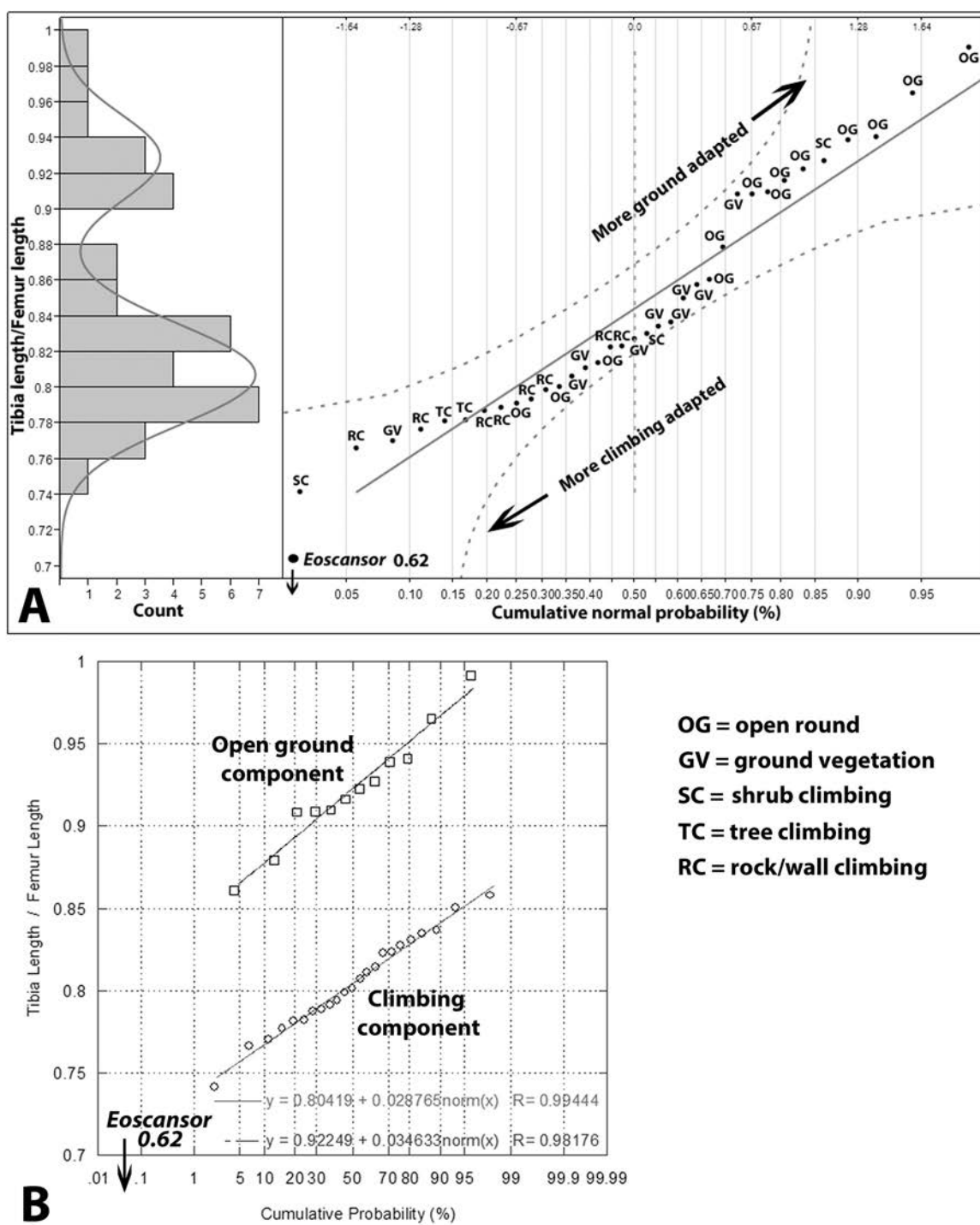


Fig. 16.—Probability plots of the tibia length/femur length (TL/FL) relationship in lizards. **A**, TL/FL distribution in 35 lizards (Appendix 1). Histogram (left) and normal cumulative probability plot with normal curve fit (solid line) and 95% confidence intervals (dashed lines) (right) show two statistically significant component distributions; one for open ground dwellers and one for lizards with some climbing capability. The data points form a stretched-S shape, and the two components can be separated at the inflection point of the S. Climbing capability increases to the lower left and open ground adaptation increases to the upper right. *Eoscaisor*, with a TL/FL = 0.62 is the most strongly climbing-adapted member of the group with respect to the TL/FL metric. **B**, probability plot of the resolved component distributions. Open ground lizards have a mean TL/FL = 0.92, $\sigma = 0.035$; climbers have a mean TL/FL = 0.8, $\sigma = 0.029$.



Fig. 17. Restoration of *Eoscansor* by Matt Celeskey.

of the terrestrial varanopid *Aerosaurus*. The manus and pes phalangeal indices are, respectively, 80.8% and 95%. These comparatively low (<100%) indices indicate a much more terrestrial adaptation.

Also, the phalangeal indices of the manus of *Anthracodromeus* (digit 3) and pes (digit 4) are low (<100%), 59% and 75%, respectively, and well within the terrestrial range. The phalangeal index of *Anthracodromeus* therefore does not indicate significant grasping capability.

Metapodial of digit I short with wide proximal end. The short, proximally widened metapodial of digit I in *Eoscansor* probably indicates a divergent digit that could assist in grasping in what has been called “pseudo-opposition.” The metatarsal of digit I has two apparent articular facets on its proximal surface (Fig. 10), and one of the metacarpals (likely from digit I) shows a similar but slightly more widened proximal end. The most parsimonious interpretation in the pes is that the two facets of the metatarsal apparently articulate with the first distal tarsal, and possibly the second distal tarsal or the lateral centrale, giving the first digit a distinct medial divergence.

The manual skeleton has a somewhat longer, proximally widened metacarpal that probably articulated with the first and second distal carpals or to the distal centrale. This

gave the digit a medial divergence similar to but less than that of digit I of the pes.

Fontanarrosa and Abdala (2016) recognized numerous grasping indicators in the manual skeletons of lizards. Among these is a widened first metacarpal. Additionally, Fröbisch and Reisz (2009, 2011) noted a widened phalangiform first distal carpal in the late Permian *Suminia* that they diagnosed as evidence of a divergent digit and a grasping adaptation. Similarly, the proximally widened first metapodials of *Eoscansor* indicate divergent digits and some grasping capability.

Relative Limb Lengths

Open ground (principally desert or semi-arid environments) lizards have long hind limbs and relatively short forelimbs, whereas climbers have shorter, nearly equal length fore- and hind limbs (Vanhooydonck and Van Damme 1999; Hildebrand and Goslow 2001). In *Eoscansor*, both the forelimbs and hind limbs are relatively short (~14% of total body and tail length, ~28% of snout-vent length) and approximately equal in length, measuring 33.3 mm and 36.5 mm, respectively. The forelimb length is 92% of hind limb length. Thus, the limb proportions of

Eoscansor do not correspond to those of ground-living lizards, but instead fit those of a climber.

Body Mass, SVL, and Robustness

For a given snout-vent length (SVL), the body mass of climbers is significantly less than that of ground-dwelling tetrapods (Meiri 2010, who cited Gans 1975); furthermore, climbers are more gracile, and the ground dwellers are more robust. We therefore undertook to compare the “robustness” of *Eoscansor* to extant lizards of known habitat. We also note that the relationship between body mass and SVL is strongly allometric because mass scales as length cubed. Therefore, only animals of similar SVL were used in the comparison.

To execute this comparison, the following data were utilized: body mass, SVL, and habitat preference of extant lizards in the SVL size range of *Eoscansor* (125 mm \pm 5 mm). These data were acquired from several sources (Vanhooydonck and Van Damme 1999; D'Cruze et al. 2009; IUCN Redlist of threatened species; Meiri 2010; Reptile Database Online) and were tabulated (Table 3). Highly derived body forms were excluded, including legless, flat bodied (horned lizards), gliders, and parachuters. Only six species from a database of more than 900 lizards met all the criteria.

To facilitate the comparison, we defined a “robustness index” in which body mass was divided by SVL, so higher numbers indicate a more robust animal and lower numbers indicate a more gracile animal. The robustness index was calculated for each species of the terrestrial, semi-terrestrial, and arboreal lizards (Table 3), and these were compared in a scatter plot (Fig. 12B). In the plot, the single completely terrestrial lizard shows the highest robustness index. Three lizards categorized as having terrestrial plus some semi-arboreal or arboreal habits show reduced robustness (two data points fall on top of each other in the plot), and the two lizards categorized as strictly arboreal or semi- arboreal are the most gracile (again, the two data points are practically the same). These differences in robustness are not small. The terrestrial plus semi-arboreal lizards are nearly twice the mass of the arboreal lizards, and the terrestrial lizard is nearly three times their mass.

Using the calculated weight of *Eoscansor* (58.3 g) and a 125 mm SVL, its robustness index is 0.47. We applied a linear curve fit to the data in Figure 12B and plotted the robustness index of *Eoscansor* on this line (filled data point). Clearly, within the constraints of this small sample *Eoscansor* allies best with the group that shows some terrestrial capability plus semi-arboreal or arboreal adaptations.

Rib Curvature

Eoscansor has gently curved ($\sim 60^\circ$ arc) to straight dorsal ribs and long gastralia, which indicate a slender body that assists the animal in assuming a tree- or surface-hugging

posture (Cartmill 1974, 1985). Such a posture would produce a lower center of gravity, which is advantageous for climbing because more weight is concentrated near the inclined substrate instead of being cantilevered away from the substrate, thus reducing stress on the limbs and claws. Therefore, the ribs and gastralia of *Eoscansor* indicate a somewhat flattened body consistent with scansorial habits.

Tibia/femur Length Ratio

In general, the tibiae of open ground cursors are elongated relative to their femora (Hildebrand and Goslow 2001). Conversely, the femora of climbers are generally longer than the tibiae, as in the arboreal pelycosaur *Ascendonautus* (Spindler et al. 2018: fig. 29). We undertook a statistical comparison of the ratio of tibia length to femur length of lizards that have known habits to see where *Eoscansor* falls on this spectrum.

Statistical testing—Using metric data from Vanhooydonck and Van Damme (1999), we calculated the tibia/femur length ratios of 35 lacertid lizards (Appendix 1). The distribution of these ratios was analyzed in a histogram to give an overview (Fig. 16A), left and, for greater detail, a probability plot with a normal (Gaussian) cumulative probability scale (Fig. 16A, right). The bimodal nature of the histogram and the long, stretched-S shape of the probability plot show that two component distributions make up the overall distribution of tibia/femur ratios (e.g., Harding 1949; King 1971). These two distributions were thus separated at the inflection point of the overall distribution and replotted (Fig. 16B). Once separated and replotted, the components show excellent straight-line fits on the normal probability scale, indicating near perfect Gaussian distribution of the data ($R = 0.982$ and 0.994 , respectively). Their resolved characteristics are: open ground distribution mean = 0.92, $\sigma = 0.035$; climbing distribution mean = 0.8, $\sigma = 0.029$.

After resolution of the two component distributions, the probability data points (Fig. 16A, right) were labeled as to the habits of the lizard species (Appendix 1), which are defined in the figure. Pertinent observations are:

1. The component distribution with the higher tibia/femur length ratio (above the inflection point, Fig. 16A, right) is largely composed of open ground animals ($\sim 85\%$).
2. The lower tibia/femur length component (below the inflection point, Fig. 16A, right) is largely composed of animals with some climbing/scrambling ability ($\sim 85\%$).
3. Nearly all open ground lizards are on the right side of the plot. Ground vegetation lizards are concentrated near the center, and the more committed climbers, SC, TC, and RC, are concentrated on the left. So, in general, climbing ability increases from right to left in the plot.
4. One of the component distributions represents more ground adapted animals, the other, more climbing adapted. The skirts of these two normal (bell-shaped) distributions overlap. Thus, a few low probability members of each

TABLE 3. Body mass, snout-to-vent length, and habitat for six lizard species with SVL = 125 mm ± 5 mm. Robustness index = body mass / SVL; higher numbers indicate more robust build, lower numbers more gracile. Habitat indicators: T = terrestrial; T+SA = terrestrial plus semi-arboreal; T+A = terrestrial plus arboreal; SA = semi-arboreal; A = arboreal. Data collected from Vanhooydonck and Van Damme (1999); D'Cruze, et al. (2009); IUCN Redlist of threatened species; Meiri (2010); Reptile Database Online.

Species	Family	SVL	Body mass (g)	Habitat	Reference to plot	Robustness index
<i>Agama caudospinosa</i>	Agamidae	130.27	82.1	T	1	0.63
<i>Laudakia lehmanni</i>	Agamidae	120.58	54.9	T+SA	2	0.46
<i>Pongona minor</i>	Agamidae	126.24	30.8	SA	3	0.25
<i>Chamaeleo senegalensis</i>	Chamaeleonidae	125	31.1	A	3	0.25
<i>Eublepharis macularius</i>	Gekkonidae	125.05	59.7	T+A	2	0.48
<i>Oplurus quadrimaculatus</i>	Opluridae	120.7	57.9	T+A	2	0.48

distribution will be found within the “boundaries” of the other. That is, any member of the ground adapted animals may possess some climbing ability and vice versa. This does not negate the fact that they are members of their climbing or ground adapted distribution and primarily behave as such.

It is interesting that the ground vegetation habitat group falls within the climber component distribution, as this supports Jenkins' (1974) observation that small tetrapods that clamber over obstructions and rough terrain show adaptations similar to climbers.

Statistical significance of the two distributions. A two-sample t-test (PAST: Hammer et al. 2001) was performed to test whether the open ground component distribution ($N = 12$) and the climbers component distribution ($N = 23$) are statistically significant populations or if they belong to a single distribution. The test showed extremely low probability that the two groups belong to the same distribution ($p = 0.003$), i.e., the two distributions are distinct and real. As mentioned above, the skirts of the bell curves of the two component distributions overlap considerably (Fig. 16, histogram), and some outliers of each distribution may be seen within the range of the other distribution. For example, one member of the ground vegetation group and one member of the shrub climbing group appear within the open ground component distribution, and three, or possibly four members of the open ground group fall within the climbing component. Ultimately, this means that even though the two component distributions can be defined with precision in terms of their means and standard deviations, an individual animal cannot be assigned with complete confidence to one of the two populations. Such an assignment can, however, be made with a high probability of correctness.

Position of *Eoscansor* on the probability plot—*Eoscansor* is the most extreme outlier ($>2\sigma$) on the left (most

climbing adapted) side of the probability plot and clearly belongs to the climbing component distribution (Fig. 16); in terms of its tibia/femur ratio, it should have been an accomplished climber.

Suminia*, *Ascendonanus*, and *Anthracodromeus—The tibia/femur length ratio of *Suminia* was calculated for comparison to that of *Eoscansor*. Data were gleaned from Fröbisch and Reisz (2009: fig. 1). Specimen numbers 1, 2, 5, and 10 were especially well exposed in this figure and were carefully measured so that their ratios could be calculated and averaged. The tibia/femur length ratio of *Suminia* is 0.79, placing it just below the center of the climbing component in Figure 16. This area of the plot is primarily occupied by the tree climbing and rock climbing lizards. In *Ascendonanus*, the femur is obviously longer than the tibia, but their lack of exposure makes precise measurements difficult. From what can be seen of the hind limbs (Spindler et al. 2018), it appears that *Ascendonanus* has a tibia/femur length ratio lower than that of *Suminia* and more similar to that of *Eoscansor*. The tibia/femur length ratio of *Anthracodromeus* is 0.58, quite low and within the scansor range (Fig. 16A). But, on the other hand, the forelimb is 75% of the hind limb length using femur-tibia and humerus-radius lengths, and 80% if the hands and feet are included. This subequal limb length argues against arboreal/scansorial habits.

Summary

To summarize, the following features indicate scansoriality in *Eoscansor*:

1. Claw curvature (92°) places it in the range of climbing reptiles and mammals.
2. Large flexor tubercles on the ungual phalanges.
3. Phalangeal index of Fröbisch and Reisz (2009) places it well within the scansorial class.
4. Elongate proximal phalanges indicate some grasping

capability.

5. First metapodial short with expanded proximal end indicating a divergent digit that suggests grasping capability.
6. Elongate penultimate phalanges indicate clinging and/or climbing capability.
7. Manual and pedal claws strongly curved.
8. Forelimb and hind limb have subequal length (fore = 33.3 mm, hind = 36.5 mm; < 9% difference).
10. Body mass estimate per Campione and Evans (2012) places it within the range of climbers for its SVL.
11. Gently curved (~60°) to straight dorsal ribs and long gastralia indicate a somewhat flattened body for tree- or surface-hugging posture.
12. TL/FL places it deeply within the climbing class (Vanhooydonck and Van Damme 1999).

With its impressive suite of scansorial adaptations, *Eoscansor* was certainly a climber, and possibly arboreal. It is essentially impossible, however, to demonstrate that it was arboreal. However, it was not likely a rock climber, given the riverine floodplain depositional setting of the El Cobre Formation from which the holotype of *Eoscansor cobrensis* was collected. This setting included lowland braided streams, small lakes, and floodplains, lush with vegetation (DiMichele et al. 2010). Several arborescent plants were present, including *Alethopteris*, *Macroneuropteris*, *Sigillaria*, and walchian conifers. *Eoscansor* could have lived in them, but there were also many shrubs and fern-like plants that it may have climbed or scrambled over (DiMichele et al. 2010). Therefore, we point out the possibility that *Eoscansor* was arboreal, but do not declare it to have been so.

CONCLUSIONS

This article supports the following conclusions:

Eoscansor cobrensis is a new genus and species of varanopid eupelycosaur.

Eoscansor cobrensis is based on an incomplete skeleton from the Cobrean (Virgilian) interval of the El Cobre Canyon Formation in the Cañon del Cobre of Rio Arriba County, New Mexico.

Eoscansor is primarily distinguished from other varanopids by the unique structure of its manus and pes metapodials and phalanges. Various features of the anatomy of *Eoscansor* indicate that it was a well-adapted scansor, the oldest such tetrapod now known (Fig. 17).

These features include: claw, phalangeal, and metapodial adaptations indicative of grasping, clinging, and climbing ability; equivalence of high claw curvature and limb length between the fore- and hind limbs; body mass per SVL within the range of extant climbing lizards; very low tibia length/femur length ratio; and a low center of gravity to facilitate an inclined surface-hugging posture. *Eoscansor* augments both the diversity and disparity of varanopids.

ACKNOWLEDGMENTS

We thank the U. S. Forest Service for a permit to collect fossils in the Cañon del Cobre, and members of the NMMNH field crews who participated in the fieldwork. Comments by an anonymous reviewer and J.R. Wible improved the content and clarity of the manuscript.

LITERATURE CITED

- ANDERSON, J.S., AND R.R. REISZ. 2004. *Pyozia mesenensis*, a new, small varanopid (Synapsida, Eupelycosauria) from Russia: "pelycosaur" diversity in the Middle Permian. *Journal of Vertebrate Paleontology*, 24:173–179.
- ANDERSON, J.F., A. HALL-MARTIN, AND D.A. RUSSELL. 1985. Long-bone circumference and weight in mammals, birds, and dinosaurs. *Journal of the Zoological Society of London (A)*, 207:53–61.
- ARETZ, M., H.G. HERBIG, X.D. WANG, F.M. GRADSTEIN, F.P. AGTEBERG, AND J.G. OGG. 2020. The Carboniferous Period. Pp. 811–874, in *The Geologic Time Scale 2020* (F.M. Gradstein, J.G. Ogg, M.D. Schmitz, and G.M. Ogg, eds.). Elsevier, Amsterdam.
- BENOIT, J., D.P. FORD, J.A. MIYAMAE, AND I. RUF. 2021. Can maxillary canal morphology inform varanopid phylogenetic affinities? *Acta Palaeontologica Polonica*, 66: 389–393.
- BENSON, R.B.J. 2012. Interrelationships of basal synapsids: cranial and postcranial morphological partitions suggest different topologies. *Journal of Systematic Palaeontology*, 10:601–624.
- BROCKLEHURST, N., R.R. REISZ, V. FERNANDEZ, AND J. FRÖBISCH. 2016. A re-description of '*Mycterosaurus*' *smithae*, an early Permian eothyridid, and its impact on the phylogeny of pelycosuran-grade synapsids. *PLoS ONE* 11(6): e0156810.
- CAMPIONE, N.E., AND D.C. EVANS. 2012. A universal scaling relationship between body mass and proximal limb bone dimensions in quadrupedal terrestrial tetrapods. *BMC Biology* 10:60; <http://www.biomedcentral.com/1741-7007/10/60>. 21p.
- CAMPIONE, N.E., AND R.R. REISZ. 2010. *Varanops brevirostris* (Eupelycosauria: Varanopidae) from the lower Permian of Texas, with discussion of varanopid morphology and interrelationships. *Journal of Vertebrate Paleontology*, 30:724–746.
- . 2011. Morphology and evolutionary significance of the atlas-axis complex in varanopid synapsids. *Acta Palaeontologica Polonica*, 56:739–748.
- CARTMILL, M. 1974. Pads and claws in arboreal locomotion. Pp. 45–83, in *Primate Locomotion* (F.A. Jenkins, Jr., ed.). Academic Press, Inc., New York.
- . 1985. Climbing. Pp. 73–88, in *Functional Vertebrate Morphology* (M. Hildebrand, D.M. Bramble, K.F. Liem, and D.D. Wake, eds.). Harvard University Press, Cambridge.
- . 1992. New views on primate origins. *Evolutionary Anthropology: Issues, News, and Reviews*, 1:105–111.
- CHRISTIANSEN, P. 1999. Scaling of the limb bones to body mass in terrestrial mammals. *Journal of Morphology*, 239:167–190.
- CLAESSENS, L.P.A.M. 2004. Dinosaur gastralia: origin, morphology, and function. *Journal of Vertebrate Paleontology*, 24:89–106.
- D'CRUZE, N., A. OLSONN, D. HENSON, S. KUMAR, AND D. EMMETT. 2009. The amphibians and reptiles of the lower Onilahy River Valley, a temporary protected area in southwest Madagascar. *Herpetological Conservation and Biology*, 4:62–79.
- DiMICHELE, W.A., D.S. CHANEY, H. KERP, AND S.G. LUCAS. 2010. Late Pennsylvanian floras in western equatorial Pangea, Cañon del Cobre, New Mexico. *New Mexico Museum of Natural History and Science Bulletin*, 49:75–113.
- FEDUCCIA, A. 1993. Evidence from claw curvature indicating arboreal habits of *Archaeopteryx*. *Science*, 259:790–793.
- . 1999. *The Origin and Evolution of Birds*. Yale University Press, New Haven.
- FONTANARROSA, G., AND V. ABDALA. 2016. Bone indicators of grasping hands in lizards. *PeerJ*, 4: e1978.
- FORD, D.P., AND R.B.J. BENSON. 2020. The phylogeny of early amniotes and the affinities of Parareptilia and Varanopidae. *Nature Ecology*

- & Evolution, 4:57–65.
- FRACASSO, M.A. 1980. Age of the Permo-Carboniferous Cutler Formation vertebrate fauna from El Cobre Canyon, New Mexico. *Journal of Paleontology*, 54:1237–1244.
- FRÖBISCH, J., AND R.R. REISZ. 2009. The Late Permian herbivore *Suminia* and the early evolution of arboreality in terrestrial vertebrate ecosystems. *Proceedings of the Royal Society B-Biological Sciences*, 276:3611–3618.
- . 2011. The postcranial anatomy of *Suminia getmanovi* (Synapsida: Anomodontia), the earliest known arboreal tetrapod. *Zoological Journal of the Linnean Society*, 162:661–698.
- GANS, C. 1975. Tetrapod limblessness: evolution and functional corollaries. *American Zoologist*, 15:455–467.
- HAINES, R.W. 1958. Arboreal or terrestrial ancestry of placental mammals. *Quarterly Review of Biology*, 33:1–23.
- HAMMER, Ø., D.A.T. HARPER, AND P.D. RYAN. 2001. PAST: Paleontological Statistics Software Package for Education and Data Analysis. 4.9.
- HARDING, J.P. 1949. The use of probability paper for the graphical analysis of polymodal distributions. *Journal of the Marine Biological Association of the United Kingdom*, 28:141–153.
- HILDEBRAND, M., AND G.E. GOSLOW. 2001. Analysis of Vertebrate Structure, 5th ed. John Wiley and Sons, Inc., New York.
- HOPSON, J.A. 2001. Ecomorphology of avian and nonavian theropod phalangeal proportions: implications for the arboreal versus terrestrial origin of bird flight. Pp. 211–235, in *New Perspectives on the Origin and Early Evolution of Birds: Proceedings of the International Symposium in Honor of John H. Ostrom* (J.H. Gauthier and L.F. Gall, eds.). Yale Peabody Museum of Natural History, New Haven.
- IUCN Red List of threatened species, Online: <http://www.redlist.org/>
- JENKINS, F.A., JR. 1974. Tree shrew locomotion and the origins of primate arborealism. Pp. 85114, in *Primate Evolution and Human Origins* (R.L. Ciochon, and J.G. Reagie, eds.). Routledge, New York.
- JENKINS, F.A., JR., AND F.R. PARRINGTON. 1976. The postcranial skeletons of the Triassic mammals *Eozostrodon*, *Megazostrodon* and *Erythrotherium*. *Philosophical Transactions of the Royal Society of London*, 273:387–431.
- KEMP, T.S. 1982. Mammal-Like Reptiles and the Origin of Mammals. Academic Press, New York.
- KIELAN-JAWROWSKA, Z., AND P.P. GAMBARYAN. 1994. Postcranial anatomy and habits of Asian multituberculate mammals. *Fossils & Strata*, 36:1–92.
- KING, J.R. 1971. Probabilty Charts for Decision Making. Industrial Press Inc., New York.
- KIRK, E.C., P. LEMELIN, M.W. HAMRICK, D.M. BOYER, AND J.I. BLOCH. 2008. Intrinsic hand proportions of euarchontans and other mammals: implications for the locomotor behavior of plesiadapiforms. *Journal of Human Evolution*, 55:278–299.
- KRAUSE, D.W., AND F.A. JENKINS, JR. 1983. The postcranial skeleton of North American multituberculates. *Bulletin of the Museum of Comparative Zoology*, 150:199–246.
- LANDMAN, N.H., R.O. JOHNSON, AND L.E. EDWARDS. 2004. Cephalopods from the Cretaceous/Tertiary boundary interval on the Atlantic coastal plain, with a description of the highest ammonite zones in North America, Part 2, Northeastern Monmouth County, New Jersey. *Bulletin of the American Museum of Natural History*, 287:1–107.
- LANGSTON, W., JR., AND R.R. REISZ. 1981. *Aerosaurus wellesi*, new species, a varanopseid mammal-like reptile (Synapsida: Pelycosauria) from the lower Permian of New Mexico. *Journal of Vertebrate Paleontology*, 1:73–96.
- LUCAS, S.G. 2006. Global Permian tetrapod biostratigraphy and biochronology. Geological Society, London, Special Publications, 265:65–93.
- . 2018. Permian tetrapod biochronology, correlation and evolutionary events. Geological Society, London, Special Publications, 450:405–444.
- LUCAS, S.G., AND K. KRAINER. 2005. Stratigraphy and correlation of the Permo-Carboniferous Cutler Group, Chama basin, New Mexico. *New Mexico Geological Society Guidebook*, 56:145–159.
- LUCAS, S.G., J.W. SCHNEIDER, AND J.A. SPIELMANN (EDS.). 2010a. Carboniferous-Permian transition in Cañon del Cobre, northern New Mexico. New Mexico Museum of Natural History and Science Bulletin, 49:12–29.
- LUCAS, S.G., S.K. HARRIS, J.A. SPIELMANN, L.F. RINEHART, D.S. BERMAN, A.C. HENRICI, AND K. KRAINER. 2010c. Vertebrate paleontology, biostratigraphy and biochronology of the Pennsylvanian-Permian Cutler Group, Cañon del Cobre, northern New Mexico. New Mexico Museum of Natural History and Science Bulletin, 49:115–123.
- LUCAS, S.G., J.A. SPIELMANN, AND K. KRAINER. 2010b. Summary of geology of Cañon del Cobre, Rio Arriba County, New Mexico. New Mexico Museum of Natural History and Science Bulletin, 49: 1524.
- LUO, Z., Q. JI, J.R. WIBLE, AND C. YUAN. 2003. An Early Cretaceous tribosphenic mammal and metatherian evolution. *Science*, 302: 1934–1940.
- MADDIN, H.C., D.C. EVANS, AND R.R. REISZ. 2006. An early Permian varanodontine varanopid (Synapsida; Eupelycosauria) from the Richards Spur locality, Oklahoma. *Journal of Vertebrate Paleontology*, 26:957–966.
- MADDIN, H.C., A. MANN, AND B. HEBERT. 2020. Varanopid from the Carboniferous of Nova Scotia reveals evidence of parental care in amniotes. *Nature Ecology & Evolution*, 4:50–56.
- MANN, A., T.W. DUDGEON, A.C. HENRICI, D.S. BERMAN, AND S.E. PIERCE. 2021. Digit and ungual morphology suggest adaptations for scansoriality in the late Carboniferous eureptile *Anthracodromeus longipes*. *Frontiers in Earth Science*, 9:675–337.
- MATTHEW, W.D. 1904. The arboreal ancestry of the Mammalia. *American Naturalist*, 38:811–818.
- MEIRI, S. 2010. Length-weight allometries in lizards. *Journal of Zoology*, 281:218–226.
- OSBORN, H.F. 1903. On the primary division of the Reptilia into two subclasses, Synapsida and Diapsida. *Science*, 17:275–276.
- PELLETIER, V. 2014. Postcranial description and reconstruction of the varanodontine varanopid *Aerosaurus wellesi* (Synapsida: Eupelycosauria). Pp. 53–68, in *Early Evolutionary History of the Synapsida* (C.F. Kammerer, K.D. Angielczyk, and J. Fröbisch, eds.). Springer Science + Business Media, Dordrecht.
- REISZ, R.R. 1981. A diapsid reptile from the Pennsylvanian of Kansas. *University of Kansas Museum of Natural History Special Publication*, 7:1–74.
- . 1986. Pelycosauria. *Encyclopedia of Paleoherpetology*, 17A:1–102.
- REISZ, R.R., D.S. BERMAN, AND D. SCOTT. 1984. The anatomy of relationships of the lower Permian reptile *Araeoscelis*. *Journal of Vertebrate Paleontology*, 4:57–67.
- REISZ, R.R., AND D.W. DILKES. 2003. *Archaeovenator hamiltonensis*, a new varanopid (Synapsida: Eupelycosauria) from the upper Carboniferous of Kansas. *Canadian Journal of Earth Science*, 40:667–678.
- REISZ, R.R., M. LAURIN, AND D. MARJANOVIC. 2010. *Apsisaurus witteri* from the lower Permian of Texas: yet another small varanopid synapsid, not a diapsid. *Journal of Vertebrate Paleontology*, 20:1628–1631.
- REISZ, R.R., AND S.P. MODESTO. 2007. *Heleosaurus scholtzi* from the Permian of South Africa: a varanopid synapsid, not a diapsid reptile. *Journal of Vertebrate Paleontology*, 27:734–739.
- RENESTO, S., AND A. PAGANONI. 1995. A new *Drepanosaurus* (Reptilia, Neodiapsida) from the Upper Triassic of northern Italy. *Neues Jahrbuch für Geologie und Paläontologie Abhandlungen*, 197:87–99.
- THE REPTILE DATABASE, Online: <http://reptile-database.reptarium.cz/>
- RINEHART, L.F., S.G. LUCAS, A.B. HECKERT, J.A. SPIELMANN, AND M.D. CELESKEY. 2009. The paleobiology of *Coelophysis bauri* (Cope) from the Upper Triassic (Apachean) Whitaker quarry, New Mexico, with detailed analysis of a single quarry block. *New Mexico Museum of Natural History and Science Bulletin*, 45:1–260.

- ROMER, A.S., AND L.W. PRICE. 1940. Review of the Pelycosauria. Geological Society of America Special Paper, 27:1–486.
- ROSE, K.D. 1990. Postcranial skeletal remains and adaptation in early Eocene mammals from the Willwood Formation, Bighorn basin, Wyoming. Geological Society of America Special Paper, 243:107–133.
- SPIELMANN, J.A., A.B. HECKERT, AND S.G. LUCAS. 2005. The Late Triassic archosauromorph *Tritylodonurus* as an arboreal climber. Rivista Italiana di Paleontologia e Stratigrafia, 111:395–412.
- SPIELMANN, J.A., S.G. LUCAS, L.F. RINEHART, AND A.B. HECKERT. 2008. The Late Triassic archosauromorph, *Tritylodonurus*. New Mexico Museum of Natural History and Science Bulletin, 43:1–177.
- SPIELMANN, J.A., S. RENESTO, AND S.G. LUCAS. 2006. The utility of claw curvature in assessing the arboreality of fossil reptiles. New Mexico Museum of Natural History and Science Bulletin, 37:365–368.
- SPINDLER, F., R. WERNEBURG, J.W. SCHNEIDER, L. LUTHARDT, V. ANNACKER, AND R. RÖSSLER. 2018. First arboreal ‘pelycosaurs’ (Synapsida: Varanopidae) from the early Permian Chemnitz fossil Lagerstätte, SE Germany, with a review of varanopid phylogeny. Paläontologische Zeitschrift, 92:315–364.
- SWOFFORD, D.L. 2002. PAUP*: Phylogenetic Analysis Using Parsimony (*and Other Methods). Version 4. Sinauer Associates, Sunderland, Massachusetts.
- UTTING, J., AND S.G. LUCAS. 2010. Palynological investigation of the Upper Pennsylvanian (Carboniferous) El Cobre Canyon Formation, Cutler Group, Cañon del Cobre, Rio Arriba County, New Mexico, U. S. A. New Mexico Museum of Natural History and Science Bulletin, 49:71–73.
- VANHOYDONCK, B., AND R. VAN DAMME. 1999. Evolutionary relationships between body shape and habitat use in lacertid lizards. Evolutionary Ecology Research, 1:785–805.
- . 2001. Evolutionary trade-offs in locomotor capacities in lacertid lizards: are splendid sprinters clumsy climbers? Journal of Evolutionary Biology, 14:46–54.
- VAN VALKENBURGH, B. 1987. Skeletal indicators of locomotor behavior in living and extinct carnivorans. Journal of Vertebrate Paleontology, 7:162–182.
- VAUGHN, P.P. 1963. The age and the locality of the Paleozoic vertebrates from El Cobre Canyon, Rio Arriba County, New Mexico. Journal of Paleontology, 37:283–296.
- ZAAF, A., AND R. VAN DAMME. 2001. Limb proportions in climbing and ground-dwelling geckos (Lepidosauria, Geckonidae): a phylogenetically informed analysis. Zoomorphology, 121:45–53.
- ZANI, P.A. 2000. The comparative evolution of lizard claw and toe morphology and clinging performance. Journal of Evolutionary Biology, 13:316–325.
- ZHENG, X., S. BI, X. WANG, AND J. MENG. 2013. A new arboreal haramiyid shows the diversity of crown mammals in the Jurassic Period. Nature, 500:199–202.

APPENDIX 1. Metric data and habitat for 35 lacertid lizards, from Vanhooydonck and Van Damme (1999).

Taxon	Habitat	SVL (mm)	Femur L	Tibia L	TL/FL
<i>Acanthodactylus aureus</i>	Ground open	50.69	11.8	10.16	0.861
<i>Acanthodactylus boskianus</i>	Ground open	61.83	13.63	12.49	0.916
<i>Acanthodactylus longipes</i>	Ground open	44.75	9.79	9.45	0.965
<i>Acanthodactylus pardalis</i>	Ground open	55.73	11.4	10.52	0.922
<i>Acanthodactylus scutellatus</i>	Ground open	48.1	9.86	9.26	0.939
<i>Eremias persica</i>	Ground open	71.57	16.71	14.69	0.879
<i>Eremias velox</i>	Ground open	64.3	14.33	11.67	0.814
<i>Ichnotropis capensis</i>	Ground open	54.72	11.01	10.36	0.940
<i>Lacerta parva</i>	Ground open	47.97	9	7.12	0.791
<i>Lacerta pater</i>	Ground open	129.03	26.37	21.12	0.800
<i>Mesalina brevirostris</i>	Ground open	53.46	10.97	9.97	0.908
<i>Mesalina guttalata</i>	Ground open	43.68	8.97	8.16	0.909
<i>Adolfus africanus</i>	Ground vegetation	54.22	11.82	9.89	0.836
<i>Adolfus jacksoni</i>	Ground vegetation	72.7	13.87	11.19	0.806
<i>Adolfus vauereselli</i>	Ground vegetation	52.3	11.06	9.49	0.858
<i>Galloptia galloti</i>	Ground vegetation	112.18	25.93	19.98	0.770
<i>Hellobolus spekii</i>	Ground vegetation	44.33	10.15	10.06	0.991
<i>Lacerta vivipara</i>	Ground vegetation	46.31	8.06	6.67	0.827
<i>Ophisops minor</i>	Ground vegetation	41.01	9.39	8.53	0.908
<i>Podarcis sicula</i>	Ground vegetation	66.36	14.52	11.78	0.811
<i>Podarcis taurica</i>	Ground vegetation	56.79	10.95	9.14	0.834
<i>Takydromus sexlineatus</i>	Ground vegetation	45.91	7.61	6.47	0.850
<i>Acanthodactylus haasi</i>	Shrub climbing	46.83	10.42	9.66	0.927
<i>Algyroides nigropunctatus</i>	Shrub climbing	57.21	11.92	8.84	0.741
<i>Lacerta viridis</i>	Shrub climbing	93.22	17.94	14.9	0.830
<i>Holaspis guentheri</i>	Tree climbing	42.17	8.1	6.33	0.781
<i>Lacerta chlorogaster</i>	Tree climbing	56.59	11.88	9.29	0.781
<i>Algyroides fitzingeri</i>	Rock/wall climbing	36.63	6.63	5.08	0.766
<i>Lacerta bedriagae</i>	Rock/wall climbing	72.22	15.31	12.23	0.798
<i>Lacerta jayakari</i>	Rock/wall climbing	126.5	30.12	23.76	0.788
<i>Lacerta oxycephala</i>	Rock/wall climbing	56.98	12.05	9.36	0.776
<i>Podarcis erhardii</i>	Rock/wall climbing	63.93	13.25	10.52	0.793
<i>Podarcis filfolensis</i>	Rock/wall climbing	73.35	14.91	12.28	0.823
<i>Podarcis muralis</i>	Rock/wall climbing	54.42	10.59	8.34	0.787
<i>Podarcis tiliguerta</i>	Rock/wall climbing	61.69	13.66	11.24	0.822

APPENDIX 2. Each of the following matrices was run in PAUP* v.4.0a169 (Swofford 2002) using parsimony analysis, run under the heuristic search option with 100 additional sequence replicates.

(continued on next page)

Maddin et al. (2020)

The parsimony analysis yielded 1,620 most parsimonious trees each with 795 steps. Wild-card taxa excluded by Maddin et al. (2020) were excluded from this analysis. *Eoscansor* was recovered as the sister taxon to *Archaeovenator hamiltonensis* in a clade diverging from the base of the Varanopidae (Appendix Fig. 1).

Eoscansor coding, Maddin et al. (2020)

????? ?????? ?????? ?????? ?????? 01020? 000??? ?????? ?2??0 00?200 01000? ??202 0?0?0 0100? 0??2?0? 10101? ?????? ?????? ?10?

Characters

8	Maxilla and dentary, medial surface adjacent to alveoli: smooth (0)
40	Lateral dentition, overall tooth morphology: conical (0)
41	Maxillary dentition, recurvature: at least slightly recurved (1)
42	Lateral dentition, cutting edges: absent (0)
44	Lateral dentition, number of apical cusps: one (0)
45	Lateral dentition, shoulder on lingual surface: absent (0)
46	Lateral dentition, labyrinthine structure: absent (1)
149	Cervical vertebrae, count: 5 or more (1)
150	Atlas-axis complex, atlantal and axial intercentra: widely separated by ventral extension of the atlantal centrum (1)
151	Axial neural spine, anteroposterior length of apex: longer than centrum (0)
152	Axial neural spine, height: tall, at least 1.5 times the height of the centrum (1)
153	Cervical centra, length: shorter than dorsal centra (0)
155	Dorsal centra, anteroposterior length: short, subequal to height (0)
158	Dorsal transverse processes: prominent but not elongate (0)
159	Dorsal transverse process, location: located anteriorly (1)
170	Dorsal ribs, curvature: curved proximally, only weakly curved distally (0)
171	Dorsal ribs, tuberculum morphology: well-developed and flange-like (0)
172	Sacral vertebrae, count: two or fewer (0)
173	Sacral rib, morphology of first sacral rib: slightly larger than more posterior sacral ribs (1)
187	Clavicle, shape of ventromedial plate: intermediate (2);
191	Interclavicle, shape of posterior margin of head: distinctly offset from shaft by posterolateral emargination (0)
192	Humerus, ridge connecting deltopectoral crest to head: double, paired ridge (0)
194	Humerus, anterior surface of deltopectoral crest: weakly concave (0)
195	Humerus, position of latissimus dorsi attachment: proximal (0)
196	Humerus, morphology of latissimus dorsi attachment: step-like transverse ridge or mound (0)
197	Humerus, posterior surface of shaft around exit of entepicondylar foramen: exit foramen large and rimmed by a longitudinal depression (1)
198	Humerus, ectepicondylar foramen: absent (0)
199	Humerus, entepicondyle, transverse width: moderate (0)
200	Humerus, ventral surface of entepicondyle: flat or weakly convex (0)
205	Manus length, McIV:radius length ratio: >0.5 (2)
206	Manus, metapodial shape: long and slender (0)
208	Manus digital formula: X3YZ3 (0)
211	Manus, phalanges, distal articular surface orientation: distal (0)
212	Manus, ungual phalanges, height:width ratio: high >1.5 (1)
213	Manus, ungual phalanges, flexor tubercle: single bulbous eminence (0)
214	Pelvic girdle, acetabulum, outline: suboval and shallow, lacking supracetabular buttress (0)
224	Femur, proportions: long and slender (1)
225	Femur, orientation of head: terminal and anteroposteriorly elongate (0)
227	Femur, mound-like eminence on dorsal surface of proximal end: small (1)
228	Femur, ventral ridge system: prominent (0)
229	Femur, intertrochanteric fossa: prominent (0)
230	Femur, posterior longitudinal ridge located proximally on ventral surface: present (1)
243	Posterior extent of anterior caudal ribs: ribs short (1)
244	Dorsal ribs, slender, proximal diameter of the shaft less than ½ centrum width (0)

Spindler et al. (2018)

The parsimony analysis limiting non-synapsid taxa to *Limnoscelis*, *Tseajaia*, and *Captorhinus* yielded 1,053 most parsimonious trees each with 515 steps. The inclusion of *Eoscansor* polarized the Varanopidae into two clades, the varanodontines and a clade including all other varanopid taxa. In the strict consensus tree, *Eoscansor* is recovered in a polytomy with *Archaeovenator*, *Ascendoranus*, *Pyozia*, *Apsisaurus*, and a clade consisting of *Mesenosaurus*, *Mycterosaurus*, and the South African varanopid taxa (Appendix Fig. 2).

APPENDIX 2. Each of the following matrices was run in PAUP* v.4.0a169 (Swofford 2002) using parsimony analysis, run under the heuristic search option with 100 additional sequence replicates.

(continued from previous page)

Eoscansor coding, Spindler et al. (2018)

0????? ?????? ?????? ?????? ?????? ?????? ?????? ?????? ?????? ?????? ?????? ?????? ?????? ?????? ?????? ?????? ?????? ?????? ?????? 00??? 101?? ?????? 20?00
01111 0????? ?????? ?????? ??101 0?010 00011 0011? ???1?1 11?0 11??? ?0

Characters

1	Dorsal osteoderms: absent (0)
99	Marginal tooth curvature: largely absent (0)
100	Marginal tooth curvature: present, but weak (0)
101	Tooth crown compression: restricted to tip or absent (0)
102	Marginal tooth serration: absent (0)
106	Axial neural spine height: tall, at least 1.5 times the height of centrum (1)
107	Cervical centra length: shorter or approximately equal to dorsal centra (0)
108	Dorsal centra anteroposterior length: short, subequal to height (0)
117	Dorsal vertebra diapophyses: relatively short (0)
119	Dorsal rib head: dichocephalous (0)
120	Dorsal rib morphology: slender (0)
121	Sacral vertebrae count: two or fewer (0)
122	Sacral ribs morphology: first sacral rib subequal to or slightly larger than second (1)
123	Clavicular ventromedial plate: expanded posteriorly (1)
124	Interclavicle head anterior process: reduced, interclavicle T-shaped (1)
125	Transition from interclavicle transverse processes to shaft: angled, producing a straight posterior border (1)
126	Transverse processes of interclavicle: defining the width of the interclavicle head (0)
143	Hind limb-trunk length ratio: hind limb almost as long or longer than trunk (1)
144	Ratio of extremities: Hind limb and forelimb subequal in length (0)
145	Femur-humerus length ratio: less than 120% (1)
146	Metapodial shape: long and slender (0)
148	Phalanges: slender (0)
149	Ungual flexor tubercle: present as a pronounced bulbous eminence (1)
150	Humerus ridge connecting deltopectoral crest to head: double, paired ridge enclosing proximolateral fossa (0)
151	Anterior surface of deltopectoral crest: weakly concave (0)
152	Position of latissimus dorsi attachment: proximal, adjacent to internal epicondyle (0)
153	Morphology of latissimus dorsi attachment: step-like transverse ridge or mound (0)
154	Posterior surface of humerus shaft around exit of entepicondylar foramen: exit of foramen very large and rimmed by a longitudinal depression, foramen only enclosed by a narrow strip of bone (1)
155	Ratio of width of distal head of humerus to humerus length: slender, less than 50% (1)
156	Entepicondyle width: moderate to large size (0)
157	Entepicondylar foramen: absent (0)
158	Radius-humerus length ratio: at least 60% (1)
159	Olecranon process: low to absent (1)
165	Manus length: metacarpal IV longer than 45% of radius length (1)
167	Femur slenderness: long and slender (1)
168	Scar for M. puboischiofemoralis internus on proximal dorsal surface of femur: inconspicuously developed (1)
170	Surface of posterior (femoral) condyle: convex (0)
171	Pes length: ratio of tibia + astragalus to metatarsal IV plus digit IV is 92% or less (1)
172	Astragalus: present (1)
177	Metatarsal IV: short, up to 50% of the length of the associated string of phalanges (0)

Ford and Benson (2020)

The parsimony analysis yielded six most parsimonious trees each with 1,565 steps. Adding *Eoscansor* to the matrix pulled the non-caseasaurian synapsids deep into the diapsid tree as a sister clade to a clade containing Varanopidae + Neoreptilia, and polarized the varanopid taxa into two discrete subclades, with *Eoscansor* nested with the varanodontines (Appendix Fig. 3).

Eoscansor coding, Ford and Benson (2020)

????? 00000 0????? ?????? 01010 0?10?
1?0?0 ?????? ?????? 000?0 0?2? ?????? ?????? ?1011 000?0 110?? ?1?1 10??? ?????? 1?1?
??1?? ?????? ?1?1

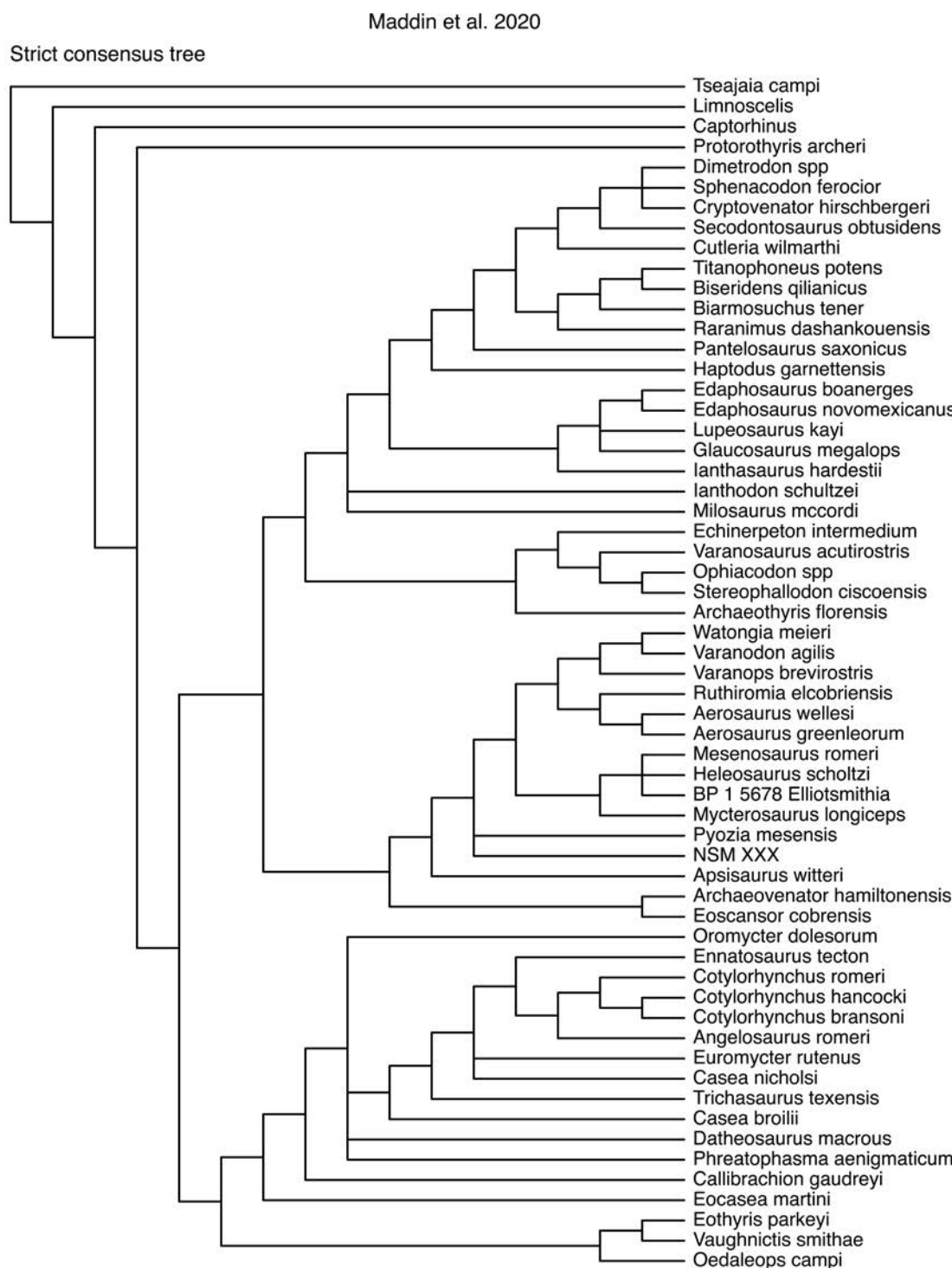
APPENDIX 2. Each of the following matrices was run in PAUP* v.4.0a169 (Swofford 2002) using parsimony analysis, run under the heuristic search option with 100 additional sequence replicates.

(continued from previous page)

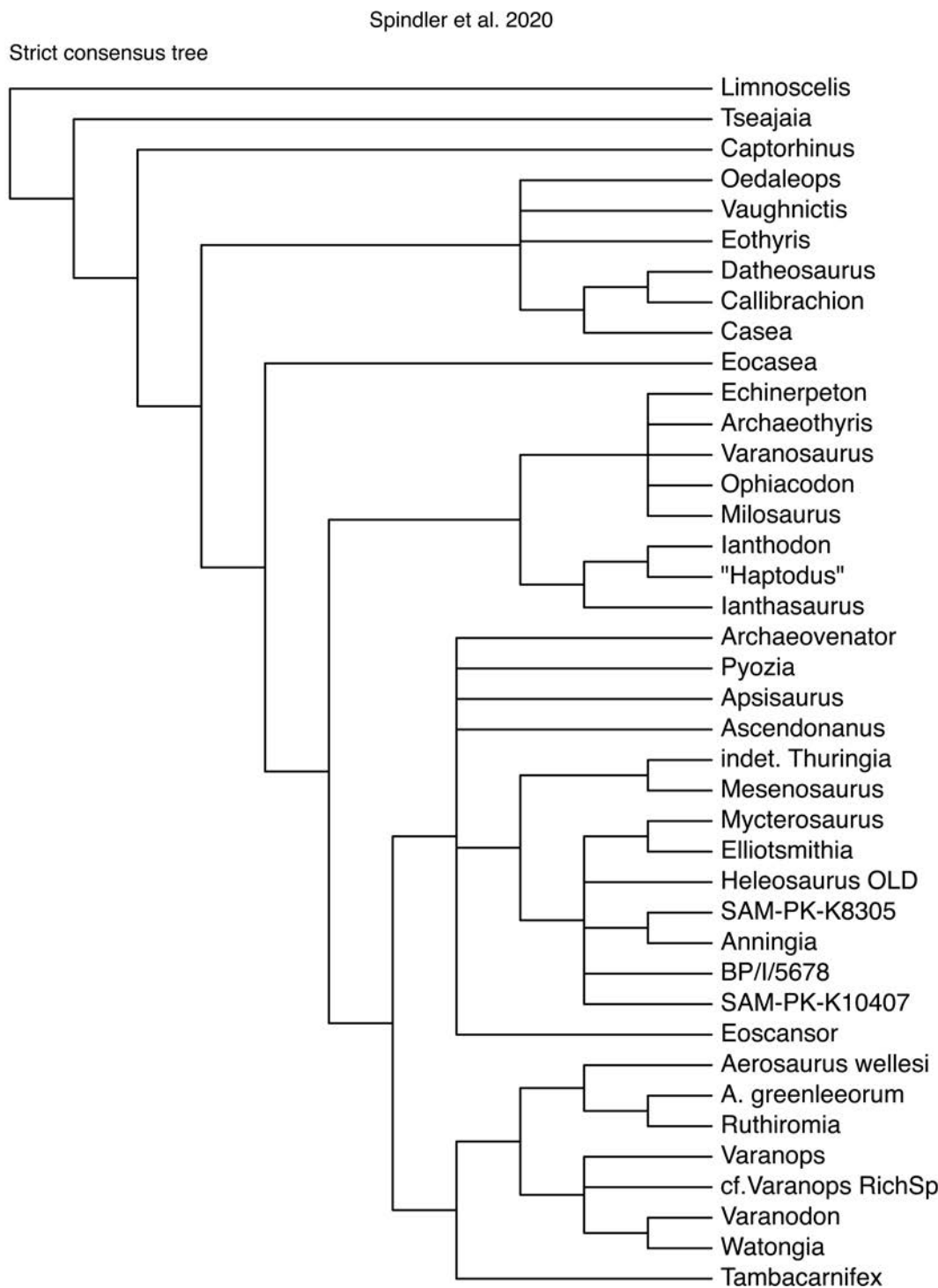
Characters

- 6 Teeth, distal curvature of marginal teeth: present (0)
- 7 Teeth, distal curvature of marginal teeth: slight to moderate (0)
- 8 Teeth, marginal dentition, cutting edges: absent (0)
- 9 Teeth, serrations on crown: absent (0)
- 10 Teeth, lateral compression of marginal dentition: only apically or nowhere (0)
- 11 Teeth, multiple apical cusps: absent (0)
- 199 Vertebrae: notochordal canal: present throughout ontogeny (0)
- 201 Cervical vertebrae, atlantal ribs: present (0)
- 202 Cervical vertebrae, atlas-axis complex, atlantal and axial intercentra: widely separated by ventral extension of atlantal centrum (1)
- 203 Cervical vertebrae, axial neural spine, anteroposterior length of apex: longer than or equal to the centrum (0)
- 204 Cervical vertebrae, axial neural spine, dorsoventral height: tall, approximately 1.5 times the height of the centrum (1)
- 205 Cervical vertebrae - ribs, slender and tapering at low angle to vertebrae: absent (0)
- 206 Cervical vertebrae, centra length: shorter than or subequal to the dorsal centra (0)
- 208 Cervical vertebrae, neural arch excavation: present (1)
- 209 Cervical vertebrae, outline of neural spines in lateral view: sub-rectangular (0)
- 211 Cervical ribs, proximal heads: all dichotomous (1)
- 213 Dorsal vertebrae, anteroposterior length of centra: short, subequal to height (0)
- 215 Dorsal vertebrae, transverse processes: short (0)
- 225 Dorsal vertebrae, trunk ribs: mostly dichotomous (0)
- 226 Dorsal vertebrae, trunk ribs, curvature: curved proximally, only weakly curved distally (0)

APPENDIX FIG. 1.—Cladistic analysis of the phylogenetic position of *Eoscaenops* using the character matrix of Madden et al. (2020).



APPENDIX FIG. 2.—Cladistic analysis of the phylogenetic position of *Eoscansor* using the character matrix of Spindler et al. (2020).



APPENDIX FIG. 3.—Cladistic analysis of the phylogenetic position of *Eoscaenior* using the character matrix of Ford and Benson (2020).

Ford and Benson 2020

Strict consensus tree

